Kaunas University of Technology
Faculty of Mechanical engineering and Design

Investigation of thin carbon and glass fibre plates impact characteristics

Master Thesis

Justas Balčiūnas
Thesis author

doc. dr. Paulius Griškevičius
Thesis supervisor

Kaunas, 2019

Kaunas University of Technology
Faculty of Mechanical engineering and Design

Investigation of thin carbon and glass fibre plates impact characteristics

Master Thesis

Mechanical Engineering(6211EX009)

Justas Balčiūnas
Thesis author

doc. dr. Paulius Griškevičius
Thesis supervisor

Assoc. prof. dr. Kazimieras Juzėnas
Thesis reviewer

Kaunas, 2019

Kaunas University of Technology
Faculty of Mechanical engineering and Design
Justas Balčiūnas

Investigation of thin carbon and glass fibre plates impact characteristics

Declaration of Academic Integrity

I confirm that the final project of mine, Justas Balčiūnas, on the topic ”Investigation of thin carbon and glass fibre plates impact characteristics” is written completely by myself; all the provided data and research results are correct and have been obtained honestly. None of the parts of this thesis have been plagiarized from any printed, Internet-based or otherwise recorded sources. All direct and indirect quotations from external resources are indicated in the list of references. No monetary funds (unless required by law) have been paid to anyone for any contribution to this project.

I fully and completely understand that any discovery of any manifestations/case/facts of dishonesty inevitably results in me incurring a penalty according to the procedure(s) effective at Kaunas University of Technology.

_____	_____
(name and surname filled in by hand)	(signature)

Kaunas University of Technology

Faculty of Mechanical Engineering and Design

Study programme: MECHANICAL ENGINERING 6211EX009

Task Assignment for Final Degree Project of Bachelor Studies

Student – Justas Balčiūnas

1) **Title of the Project –**

Investigation of thin carbon and glass fibre plates impact characteristics

(In English)

Plonasienių anglies ir stiklo pluošto plokštelių smūginių charakteristikų tyrimas

(In Lithuanian)

2) **Aim and Tasks of the Project –**

To investigate and compare impact properties of commonly used thermoset(epoxy) and novel thermoplastic(PMMA) composites. Investigate manufacturing capabilities of novel PMMA resin.

3) **Initial Data –**

Carbon and glass fibre, epoxy resin mechanical properties.

4) **Main Requirements and Conditions –**

Conduct experiments for epoxy and PMMA resin specimens at identical conditions.

Project author

(Name Surname)	*(signature)*	*(date)*

Supervisor

(Name Surname)	*(signature)*	*(date)*

Programme Director of the Study field

Assoc. Prof. Kęstutis Pilkauskas		
(Name Surname)	*(signature)*	*(date)*

Table of Contents

List of Figures

List of Tables

Abbreviations

1) PMMA - Poly(methyl methacrylate)
2) FEM - FInite Element Method
3) PAN - Polyacrylonitrile
4) SEM - Scanning Electron Microscope
5) PP - Polypropylene
6) MFA - Microfibrilis Angle
7) ROM - Rule Of Mixtures
8) SFFT - Single Fibre Fragmentation Test
9) NDT - Non-Destructive Testing
10) UD - Uni-directional (referring to fibre orientation)

Summary

Justas Balčiūnas. Investigation of thin carbon and glass fibre plates impact characteristics. Master's Thesis / supervisor doc. dr. Paulius Griškevičius; Faculty of Mechanical engineering and Design, Kaunas University of Technology.
Study field and area (study field group): Mechanical Engineering(6211EX009).
Keywords: Thin-walled, Composites, low speed impact, thermoset, thermoplastic, glass fibre, carbon fibre, epoxy, PMMA, temperature effects.
Kaunas, 2019. 50 p.

In this paper a study on impact properties of thin UD carbon and twill weave glass fibre laminates produced with novel PMMA resin produced by Ottobock compared to laminates produced with one of the most commonly used resins in the composite industry - epoxy. The properties evaluated are the maximum impact force with the corresponding absorbed energy values as well as force and energy values at damage initiation and penetration occurrence. The tests are performed on a Magnus 1000 impact testing machine in four different temperatures - room temperature, 40°C, 60°C, 80°C. The results reveal the strengths and weaknesses of the novel thermoplastic resin system from which recommendations can defined with regard to its suitability as a more sustainable alternative to epoxy resin system.

Santrauka

Justas Balčiūnas. Plonų anglies ir stiklo pluošto plokštelių smūginių charakteristikų tyrimas. Magistro baigiamasis projektas / vadovas doc. dr. Paulius Griškevičius; Kauno technologijos universitetas, Mechanikos Inžinerijos ir dizaino fakultetas.
Studijų kryptis ir sritis (studijų krypčių grupė): Mechanikos inžinerija(6211EX009).
Reikšminiai žodžiai: Ploniasieniai, kompozitai, mažo greičio smūgiai, stiklo pluoštas, anglies pluoštas, epoksidinė derva, PMMA, temperatūriniai efektai.
Kaunas, 2019. 50 p.

Šiame darbe aptariamos ir palyginamos vienakrypčio anglies pluošto ir pinto stiklo pluošto laminatų pagamintų su naujo tipo PMMA termoplastine derva(gamintojas Ottobock) ir įprasta epoksidine derva, smūginės charakteristikos. Nagrinėjami tokie parametrai kaip maksimali atlaikyta jėga ir šią jėgą atitinkanti sugerta smųgio energija. Taip pat analizuojama jėga bei energija metu, kai kompozite užfiksuojama pirma žala bei kompozitas yra pramušamas. Bandymai yra atliekami Magnus 1000 smūgine bandymų mašina keturose skirtingose temperatūrose - kambario, 40°C, 60°C, 80°C. Rezultatai atskleidžia stipriasias ir silpnasias, kompozitų pagamintų su naujovišku PMMA termoplastiku, savybes. Tuo remiantis yra pateikiamos rekomendacijos, kokiomis sąlygoms esant šis termoplastikas galėtų būti tinkamas pakaitalas epoksidinei dervai.

Introduction

Composite materials are now widely used across many industries including automotive, medical and aviation. In such applications it is important to not only have high performing materials for the parts but also ones that can be recycled. In the European Union car manufacturers are pushed to design and manufacture cars in such a way that high recyclability of the parts at the end-of-life cycle is achieved. Here opportunity arises to use novel thermoplastic resins to be used instead of conventional thermoset resins. In recent years there have been a lot of research conducted in the area of these materials especially in attempts to manufacture thermoplastic resins that could be used with conventional manufacturing methods used nowadays, hence easing the transition for the companies. In the present research a novel PMMA type resin manufactured by Ottobock (serial number 617H19) is chosen to be compared to conventional epoxy resin specifically in terms of impact resistance. The paper consists of a brief overview on the mechanics of the composites as well as fracture mechanics related to the topic. Followed by the tests to determine the common mechanical properties for this novel material. Lastly carbon composite panels with both resin types are tested using high speed impact tower. The results from the tests are used to characterize the differences between the two resin types and discuss the possible application possibilities and limitations of the PMMA resin manufactured by Ottobock.

1. Literature review

Analysis of the composites is a complex matter and thus a vast understanding on the different aspects of composites constituents is required in order to make correct assumptions and conclusions when conducting research. This literature review will cover basic overview on the microstructure of the most commonly used fibres will be provided - namely carbon, glass and cellulose fibres. The chapter will also cover brief comparison between the two resin types used in the composites - thermoplastic and thermosets, their differences and motivations to use each one of them. Moreover, stress transfer in composites and major failure mechanisms in the composites will be covered as they are crucial for the conducted research on impact resistance. Lastly, composites recycling is discussed in terms of motivation and future forecasts.

1.1. Carbon fibres

When talking about carbon fibres one must first understand the underlying microstructure which determines the mechanical properties "ceiling" that can be achieved using various fabrication techniques covered in the following chapter. Carbon is the sixth lightest element on earth and C-C covalent bond is the strongest in nature – 4000 kJ/mole [11]. Of course, the strength of the bond can vary according to the spacing of the atoms and thus several forms of carbon can be found including graphite, graphene or diamond.

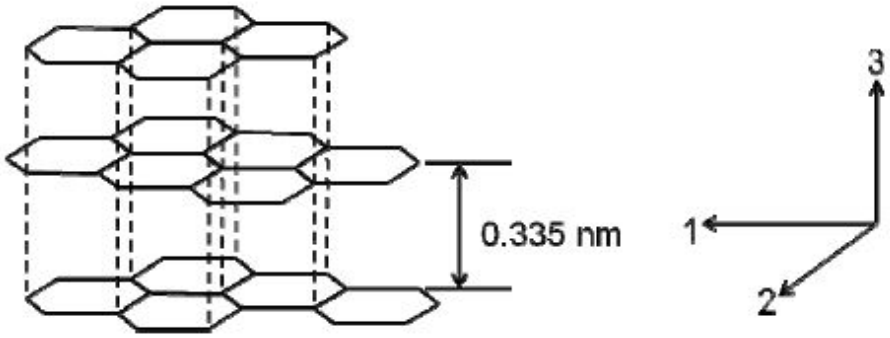

Fig. 1.1 Graphitic crystal [12]

In figure 1.1 a graphitic structure is displayed. It consists of carbon atoms arranged in regular hexagonal pattern with strong covalent bonds between them. Such arrangements in plane are called graphene sheets. They are held together with much weaker Van der Waal's forces [12]. Such atomic force distribution explains why carbon fibres have much higher strength and stiffness in the preferred (covalent bonds) direction.

The distance between two perfectly aligned graphene sheets is 0.335 nm although this distance can be bigger in carbon fibres. This is because the atomic structure in carbon fibres is not perfectly graphitic (meaning aligned in parallel to each other) but rather turbostratic. Such structure consists of stacks of graphene layers oriented in irregular pattern with angles of up to 180 degrees to one another [13].

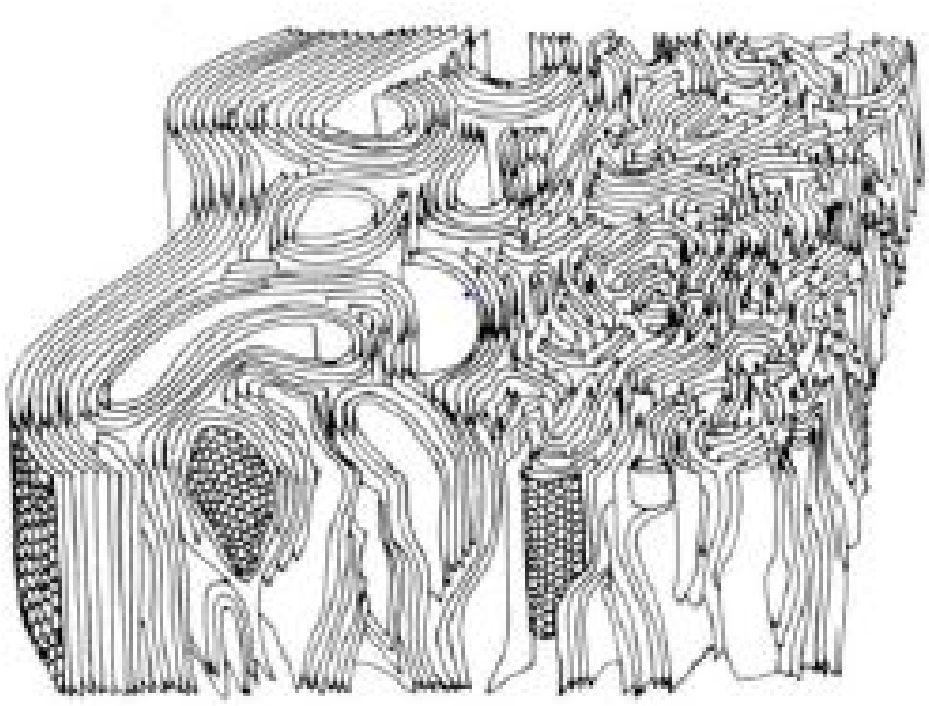

Fig. 1.2 Turbostratic graphene layers orientation in carbon fibres [13]

However the level of alignment differs depending on the precursor used - Pitch based carbon tend to have well oriented graphene basal planes while PAN tend to have more randomly oriented basal planes. As stated previously the strength of the carbon fibre comes mainly from the strong covalent bonds between the carbon atoms in the basal planes. It is thus easy to understand why carbon fibres with more aligned (graphitic) microstructure has higher modulus in the preferred direction than fibres with predominantly turbostratic microstructure - more strong covalent bonds in the loading direction will require more energy to dislocate the atoms.

As for the strength of the fibres it is governed by the crystaline morphologies and defects [12]. Comparing PAN and Pitch type carbon fibres according to this criteria it is evident why former tend to have higher strength than the later. Carbon fibres produced using petroleum pitch as a precursor tend to have better aligned but also bigger crystal sizes compared to fibres produced from PAN precursors. Bigger crystal size will inherently be more susceptible to defects which explains why Pitch-based carbon fibres tend to have lower strength.

Table 1.1 Typical carbon fibre mechanical properties [11]

Carbon fibre type	PAN HS	PAN HM	Oil-derived pitch	Oil-derived pitch HM	Coal tar pitch	Coal tar pitch HM
Density (g/cm^3)	1.82	1.94	2.1	2.16	2.12	2.16
Strength (20°C)(GPa)	7.1	3.92	3.7	3.5	3.6	3.9
Elastic modulus (20°C)(GPa)	294	588	390	780	620	830
Failure strain (20°C)(%)	2.4	0.7	0.9	0.5	0.58	0.48

1.2. Glass fibres

The other type of fibres commonly used in the industry are the glass fibres. In fact over 90% of all fibre reinforced composites are manufactured using glass fibres [14]. Glass fibres have been first introduced to the industries in the first half of the $19th$ century by the American companies of Owen Illinois Glass Co. and Corning Glass Works. The glass fibres nowadays are fabricated by melting the raw materials in a furnace. Molten glass then goes into platinum bushing or similar apparatus and divides the molten glass mass into separate streams which then gets collected at the next operational step. At this step size is also reduced to the specification which is usually around 14μm. Although the diameter can vary depending on the manufacturing process and the thinner fibres tend to be stronger due to comparatively smaller outer surface area having less flaws. The last operation is then for the fibre in correct diameter to be wound on a collet. Very importantly the fibre is also coated with a special outer coating called ”sizing” which is usually falls in the weight range of $0.2 - 2\%$ of the complete fibre weight. The purpose of this coating is two-fold - protect the fibres from mechanical damage (i.e. scratching, denting) and on the application side to provide better chemical bonding properties with the matrix polymer when used in composites laminates manufacturing. The protection part is very important as the strength of the fibres hugely depends on the size of the surface flaws.

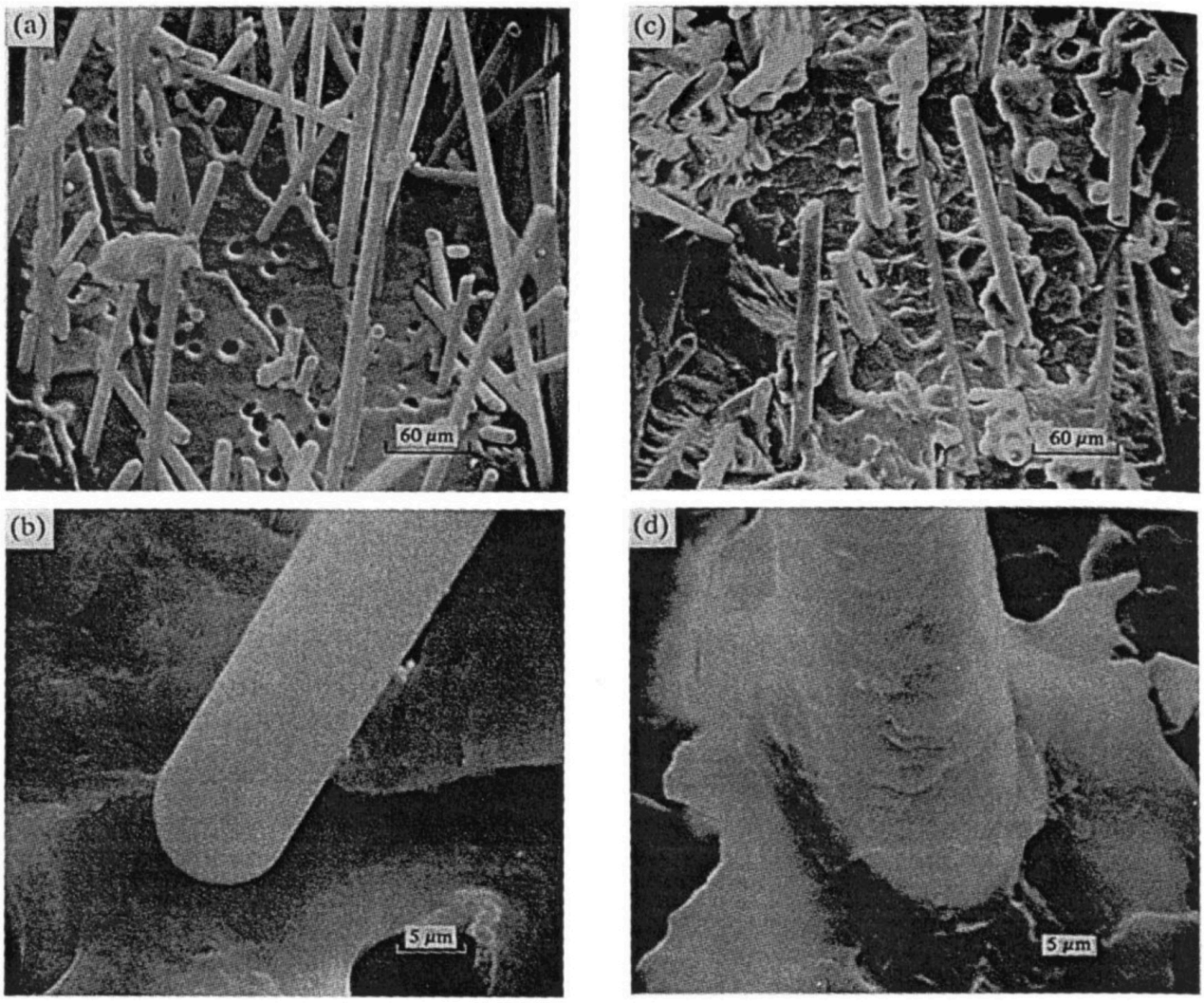

Fig. 1.3 SEM micrograph of fracture surfaces of PP/glass fibre composite. The glass fibres in a) and b) has not been applied with sizing while fibres in c) and d) have been. Shorter pull out lengths and and better adherence indicate higher bond strength between polymer and fibres with sizing applied.

Below in the table 1.2 the properties for the most commonly used glass fibre types are listed. In addition to having slightly different properties these varieties of glass fibre all have their specific areas of application [16]:

- E-glass - Electrically resistant glass fibres, most commonly used as a general purpose glass fibre.
- S-glass - High strength variation of E-glass developed for airspace industry.
- R-glass - High strength and high modulus glass fibre, less expensive than S glass.
- C-glass - Glass fibre with improved durability and corrosion resistance.
- D-glass - Fibres with improved dielectric properties and lower density by the cost of reduced mechanical properties.

Table 1.2 glass fibre varieties mechanical properties [16]

Glass type	E	S	R	C	D
Density (g/cm^3)	2.54	2.49	2.49	2.49	2.16
Strength (20°C)(GPa)	3.5	4.65	4.65	2.8	2.45
Elastic modulus (20°C)(GPa)	73.5	86.5	86.5	70	52.5
Failure strain (20°C)(%)	4.5	5.3	5.3	4.0	4.5

1.3. Cellulose fibres

In addition to carbon and glass fibres, the third type of fibres commonly used in the industry are the cellulose fibres. An example of such fibres is flax, hemp or jute. The motivation of using such fibres is that they have comparable mechanical characteristics to the glass fibres while being ”eco-friendly”. The cellulose fibres by themselves have a composite structures consisting of cellulose microfibrilis embedded in the matrix of lignin and hemicellulose.

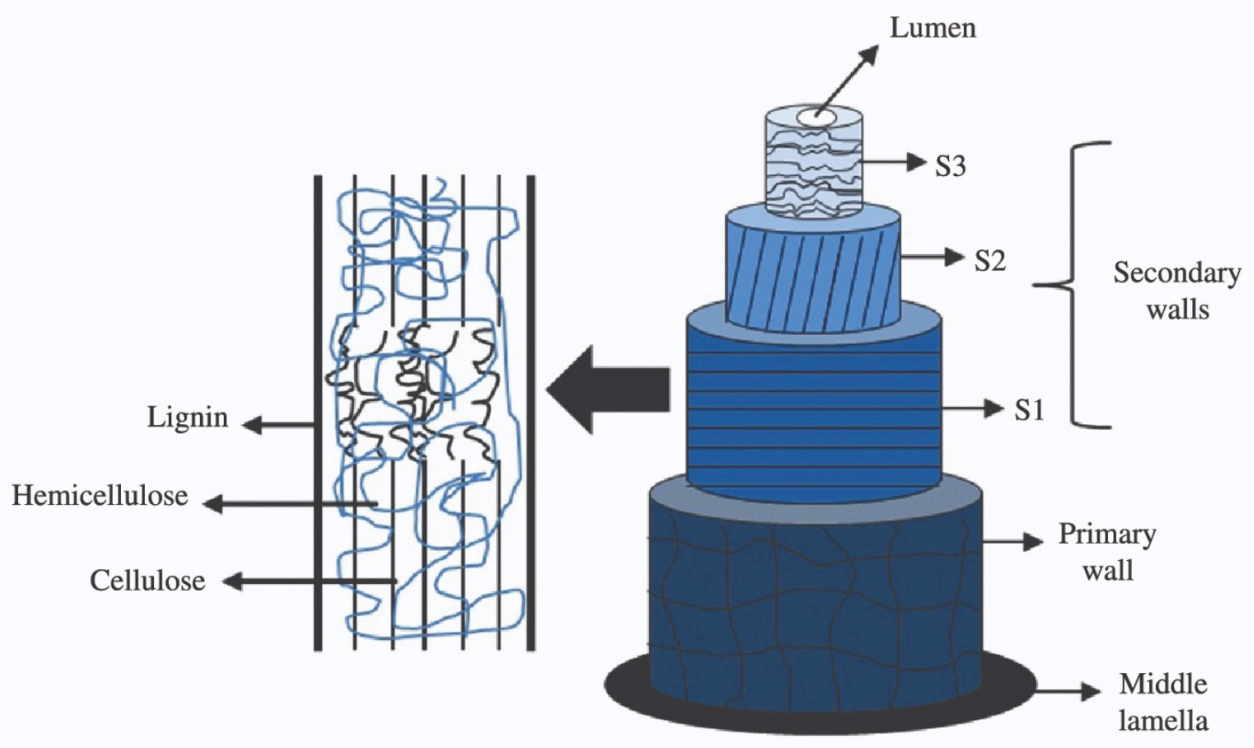

Fig. 1.4 Cellulose fibre microstructure. Represented are the cellulose wall layers in each of which microfibrilis are embedded in lignin and hemicellulose matrix.

As shown in the figure 1.4, the cellulose fibre consist of several layers. In these layers cellulose which is the primary component determining the mechanical properties of the fibre is orientated at varying angles. The wall layer denoted as ”S2” and its cellulose Microfibrilis Angle(MFA) is thus re-

sponsible for the strength of the fibre. The aforementioned MFA is the key difference when comparing different cellulose fibre varieties. For example MFA for of Hemp plants are 6% while for Cotton it is 25%. Such differences are the reason why Hemp fibres are significantly stiffer than Cotton. Furthermore, the cellulose fibres are partly amorphous as visualized in the figure 1.4 by the part straight part curly cellulose lines. The physical meaning of the crystalinity is that if it is 100% it would be expected to achieve theoretical strength values related to cellulose chains bond strength (if idealized scenario with no flaws is assumed). Normally, however, it is less than 100% but is a good measure to characterize and compare different cellulose fibres. Lastly, the cellulose fibres have fairly high water absorption due to its microstructure - inner porosity (Lumen). This is in contrast to glass fibres which absorb nearly no water(moisture) from the atmosphere.

Table 1.3 Cellulose fibre properties [17], [18]

Cellulose fibre type	Hemp	Flax	Jute	Sisal	Cotton	Softwood
Density (g/cm^3)	1.5-1.6	1.5-1.6	1.3-1.5	1.2-1.4	1.5-1.6	1.2-1.4
Strength (20°C)(GPa)	0.3-0.8	0.5-0.9	0.2-0.5	0.1-0.8	0.3-0.6	0.1-0.17
Elastic modulus (20°C)(GPa)	30-60	50-70	20-55	9-22	6-10	10-50
Crystallinity ($\%$)	79.9	86.1	58	72.2	74	71.6

1.4. Matrix

Two main types of matrix types are currently used in the industry - thermoset and thermoplastic. Various thermoset resins such as epoxy or polyester have been used in the composite industry for decades. In its uncured form thermosetting resin has a fairly low viscosity which is beneficial for impregnation of the fibres during composites manufacturing. It is cured by introducing a hardening agent which cross-links the epoxy polymers - a reaction that can be accelerated by heat. Curing cycles can range several hours to as long as 12 hours depending on post processing temperature and time. A schematic representation of the chemical curing process is shown in figure 1.5. The advantages of using thermoset type resins is their excellent mechanical properties to weight ratio, easy forming and cost effectiveness. Moreover, they are very resistant to corrosion, they have low water absorption, low thermal conductivity and good dielectric properties. All of which makes it an excellent choice for among other marine and aviation industries. However, it does not come without disadvantages - namely brittleness, no effective way of being recycled, unable to be reshaped or healed after hardening.

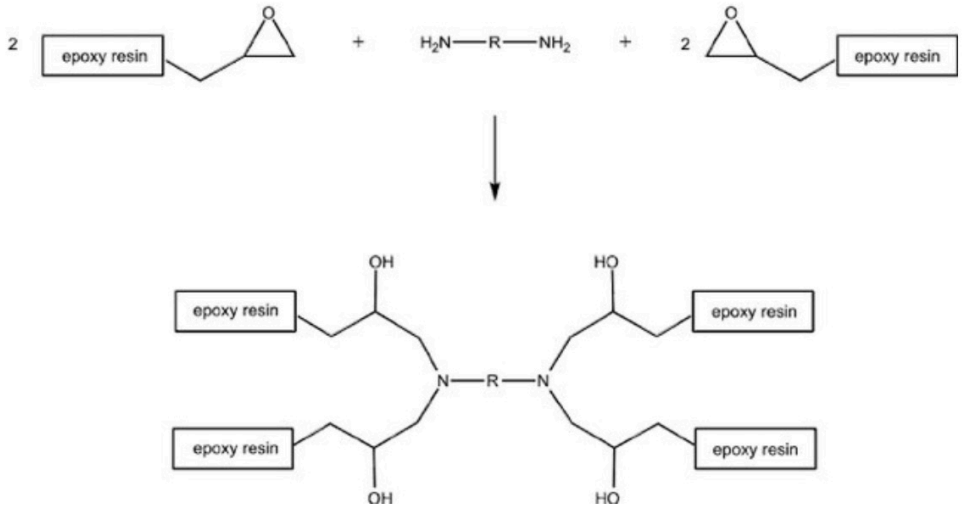

Fig. 1.5 Simplified schematic representing curing reaction between epoxy resin polymer and polyamine hardener [19]

Thermoplastics, on the other hand solve some of the issues with the thermoset resins - they have the ability to be reshaped, remolded and recycled. Such qualities for the common thermoplastic materials are by design as in their natural form they are solid rather than liquid and only by the application of heat they liquefy and can be molded into shape or impregnate fibres during composite manufacturing. This until recently have meant that completely different manufacturing methods to thermoset resin would have to be used. It is a significant disadvantage as tooling and manufacturing process change costs renders usage of thermoplastics for the composite manufacturing very limited. Recently there have been developed new types of thermoplastic resins that are liquid in their natural state. Examples of such resins are Elium by Arkema and Ottobock's PMMA thermoplastic resin range. These novel resins retain the traditional thermoplastic advantages such as ability to be reformed and recycled by dissolving back into Methyl methacrylate monomers. At the same time identical manufacturing processes as for thermosets could be used easing the possible transition for the companies. Before that happens more studies have to be performed to characterize these novel thermoplastic resins and identify if they are suitable replacement for the common thermosets.

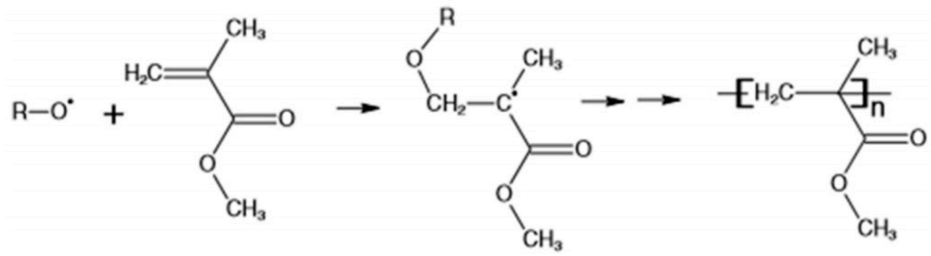

Fig. 1.6 Simplified schematic representing polymerisation reaction from Methyl methacrylate monomer to Poly Methyl methacrylate with peroxide initiator [20]

1.5. Stress transfer

Important concept to understand when discussing the fracture mechanisms within composites is the stress transfer between the two phases. First, when looking at the continuous fibres embedded in matrix - if idealized arrangement is assumed when both phases are perfectly parallel to one another, spanning entire composite length, then it can be easily proven that there is no stress transfer between the constituents. In such parallel configuration the strains are equal, hence $\epsilon_c = \epsilon_m = \epsilon_f$. Following the same logic the external load will be distributed between the phases according to their cross sectional area $P_c = P_f + P_m$, where $P = \sigma A$. The resulting equation is then $\sigma_c A_c = \sigma_f A_f + \sigma_m A_m$. In the following simplified Rule Of Mixtures (ROM) model with no porosity and perfect elasticity is assumed, stress σ is expressed with Hooke's law with strains being equal as explained previously - $E_c \epsilon_c A_c = E_f \epsilon_c A_f + E_m \epsilon_c A_m$. Next, the fractions $A_{f/m}/A_c$ are expressed in terms of fibre volume fraction ($v_f/v_c = A_f/A_c$, analogously for matrix) yielding the equation:

$$E_c = V_f E_f + V_m E_m \tag{1.1}$$

From this equation one can easily express the distribution of load between the fibres and matrix:

$$\frac{P_f}{P_c} = \frac{V_f E_f}{E_c} \tag{1.2}$$

The stress transfer between composite's constituents is more complicated when discontinued fibres are analyzed - i.e. chopped fibre laminae or fractured continuous fibres. The two main theories regarding this subject are the Elastic model (Cox 1952) [9] and the Constant Shear Stress model (Aveston, Kelly, 1973) [10]. Both models predict maximal interfacial shear stresses close to the fibre ends, decreasing to minimum values towards the fibre middle point. The tensile stress, however, is assumed zero at the fibre ends, increasing towards maximal value at the fibre middle point.

The elastic model is valid with the assumptions that fibres and matrix are elastic with fibre stiffness being higher than that of matrix. Moreover, perfect adhesion between matrix and fibre is assumed as well as local shear deformation in matrix near the fibre and tensile deformation far away from the fibre and in the fibre. The typical model graphs are presented below in the figure 1.7.

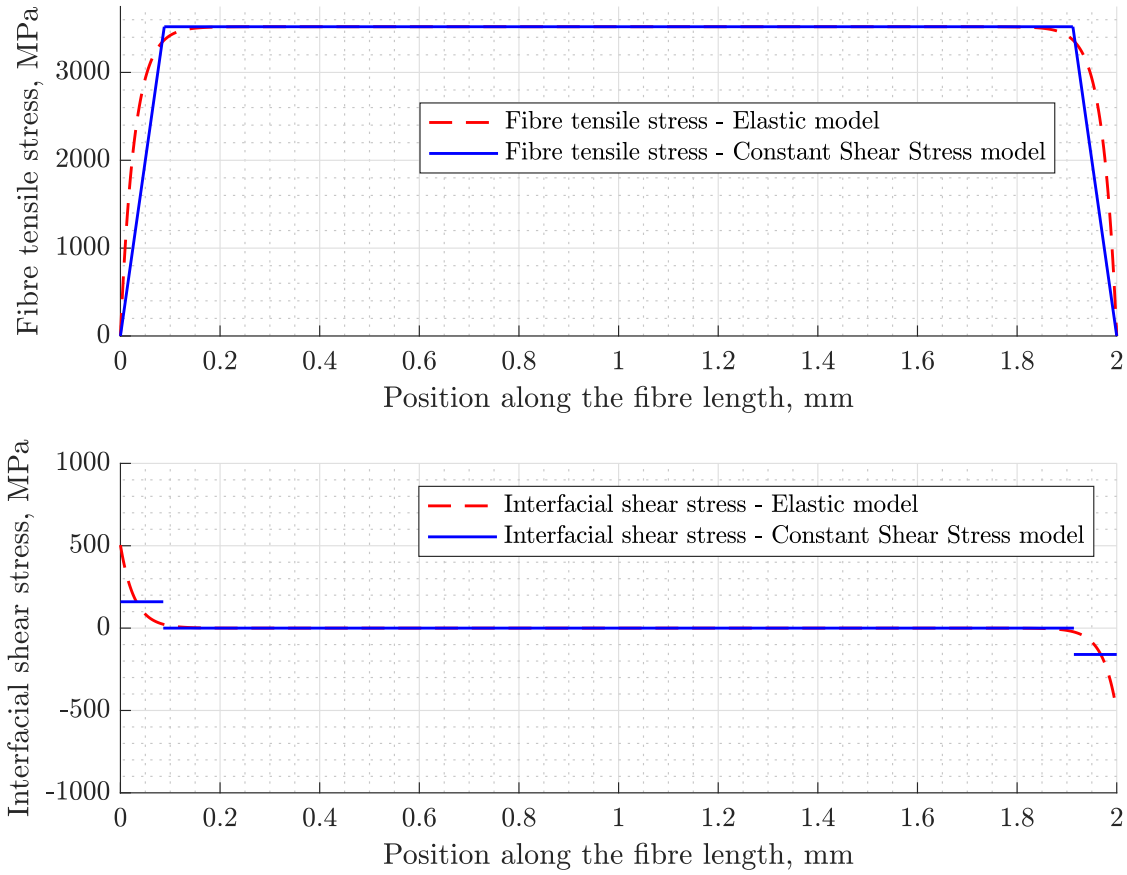

Fig. 1.7 Fibre tensile and interfacial shear stress distribution along the length of short fibre according to Elastic and Constant Shear Stress models. Values are arbitrary.

Both of the models agree that at a certain point (determined by the properties of matrix and fibre) the tensile stresses reach their maximal value and remain constant while interfacial shear stresses at the same point become zero (stress is transferred from matrix to fibre). If fibre is sufficiently long the maximal stress in the fibre is equal to so-called ideal stress in the fibre $\sigma_{f,ideal} = E_f e$. A parameter called fibre length factor predicts how well the stress is transferred in the composite system - $\eta_L = \frac{\bar{\sigma}_f}{\sigma_{f,ideal}}$. It is influenced by the properties of the matrix and fibres - decrease in matrix shear modulus will heavily decrease the fibre length efficiency factor. This means that during loading less of the stress is taken up by the fibres and consequently failure occurs sooner. Somewhat surprisingly the increase in fibre tensile modulus will result in decrease of the fibre length efficiency factor. That would imply that chopped glass fibre reinforcements are more effective that respect than their carbon counterparts. The Constant Shear Stress model addresses one of the problems with the Elastic model - unreasonably high predicted shear stresses at the fibre ends. Logically these stress cannot exceed tangential stresses at which the material fails. In this model shear stresses are assumed constant and have values of 0 and τ_0 (shear strength) depending if frictional slip or yielding is present. The distance

required for the stress to build up to maximal value is termed the Stress transfer length:

$$l = \frac{\sigma_{f,max}}{4\tau_0} d \tag{1.3}$$

$$l = \frac{\sigma_{fu}}{2\tau_0} d \tag{1.4}$$

Where τ_0 is the interfacial shear strength. It is visually represented in the figure 1.8.

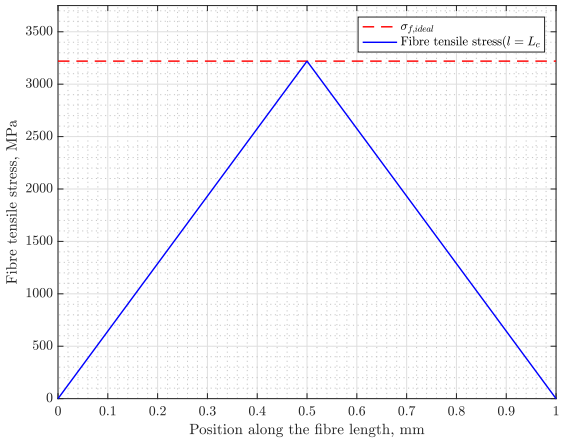

Fig. 1.8 Tensile stress distribution along the fibre length when $l = L_c$.

As it can be seen from the figure above the maximal stress or the fibre failure stress can only be achieved when the fibre length is equal or bigger than $2l = L_c$. Such mechanism is taken advantage of during Single Fibre Fragmentation Test(SFFT). In this test tensile stress is applied on test specimen with single embedded fibre. The fibre fractures in multiple fragments, all of them in the range of $0.5L_c - L_c$. The mean of the fragments is related to the critical length as follows:

$$\bar{L} = 0.68 L_c \tag{1.5}$$

The calculated L_c value can then be used to calculate the interfacial shear strength.

1.6. Failure mechanisms of composites

Contrary to commonly used engineering materials that have a single phase on macro scale, composites are by definition comprised of two or more distinct phases. Such arrangement dictates the variety of possible failure mechanisms that can be observed in composite structures. The energy is considered to be dissipated or absorbed when elastic energy stored in the material is converted to another type of energy. For example a snapped fibre may exert an acoustic wave or the creation of the new surfaces may result in kinetic energy transformation as the inter-atomic forces are broken off. Additionally a significant amount of energy is dissipated through thermal energy transformations due to friction between debonded fibres and matrix. In the following section the major composites' fracture mechanisms will be detailed.

1.6.1. Fibre-matrix debonding

Fibre-matrix debonding is usually the first fracture mechanism to be initiated. When an external stress field is applied on the system its energy is increased. It is elastically deformed until the stored strain energy equals energy to create two new surfaces i.e. a crack. Such failure usually first takes place in the matrix due to it being weaker compared to the fibre phase as well as where the flaws (voids) are. Once the crack is initiated it has several possibilities for propagation - either to continue in a straight line i.e. fibre fracture or deflect and continue parallel to the fibre along the interface. The path is dependant on the fracture energies of the interface and the fibre. The relation can expressed as follows [1]:

$$\frac{G_d}{G_p} \geqslant \frac{G_{ic}}{G_{fc}} \tag{1.6}$$

Where G_d is the energy release rate for debonding between fibre and matrix; G_p - energy release for penetrating crack; G_{ic} - fracture energy of the interface; G_{fc} - fracture energy of the fibre. Thus from equation 1.6 comes two conditions for crack deflection (debonding) occurrence - the interface should be sufficiently weak so that energy release rate for debond crack would be higher than interface fracture energy and simultaneously the energy release rate for penetrating crack would be smaller than fracture energy of the fibre. Such conditions ensure that fibre does not fracture and the only energetically favourable path for the crack is to deflect parallel to the fibre through the interface. Weaker interface will result in longer debond lengths and thus increase in dissipated crack energy. It, however, does not imply that with infinite weak interface the dissipated energy will be the highest as at certain point the interface will be so weak that the composite will exhibit extensive fibre pull-out and debonding without significant increase in dissipated energy [6]. Debonding is seen as a toughening mechanism for the composites as the materials fails in less sudden (brittle) manner resulting in less catastrophic failure which is desirable in most applications. However such failure type could at times be difficult to observe by eye especially after low energy impacts. It is important to know as the properties of the material may have reduced. For such purpose many Non Destructive Testing (NDT) techniques are available E.g. Ultrasonic, Acoustic Emission.

The interface debond energy equation has been expressed by Outwater and Murphy [5] and is as follows:

$$G_{id} = 4V_f \frac{l_d}{r} G_{ic} \tag{1.7}$$

Where V_f is the fibre volume fraction; l_d - debonded length; r - fibre radius; G_{ic} - interface fracture energy (depends on materials).

1.6.2. Fibre fracture

Fibre fracture generally leads to a catastrophic failure of the entire composite. The fibre penetration(fracture) occurs when the energy release rate of fibre penetrating crack is higher than fracture

energy of the fibre [1]:

$$G_p > G_{fc} \tag{1.8}$$

The fracture energy itself is related to strain energy stored in the fibre, or $w = \sigma\epsilon$ and if it is assumed that the fibre and the matrix is bonded together, then the strain ϵ is constant in the entire composite including the fibres then the fracture energy per fibre is directly related to its ultimate strength σ_{fu}. The ultimate strength in fibre is very much dependant on the surface and volume flaws as well as crystallinity. Multiple fibres even from the same batch will have vastly different strength values. As the fibres begin to break, localized stress concentrations will begin to occur that in turn increases the likelihood of adjacent fibres fracturing. The practical meaning of such behaviour is that once fibres start fracturing at some point within the composite, it will likely continue to quickly grow in one direction due to stress concentrations. Therefore, fibre fracture can be associated with brittle composites. Another process associated with the fibre fracture is fibre shear failure as reported in Composite materials handbook. It has been discussed in the previous chapter that as fibre fracture the stress is being transferred to the newly created two fibres by the shear stress within matrix and fibre interface. This feature hugely depends on the combination on fibres and matrix used but in some cases weaker interfacial shear strength may be beneficial as debonding will arrest the propagation of fibre cracks and thus less of a catastrophic failure model may be achieved.

1.6.3. Fibre pull-out

Fibre pull-out occurs as a result of fibre fracture. Due to stress concentrations close to the fractured fibre an opening in the matrix is initiated. The frictional interfacial shear stress behind the crack front resists the crack opening. The force balance for the fibre pulled out of the matrix can be expressed as follows:

$$\sigma_f \pi r^2 = \tau_s 2\pi r(l_0 - \delta) \tag{1.9}$$

where σ_f is the applied stress on the fibre behind the crack front, r-fibre radius, τ_s-interfacial shear stress, l_0 - pulled out fibre length, δ - matrix crack opening.
Expressing the fibre stress with far-field stress, fibre volume fraction and rearranging the terms, one gets:

$$\bar{\sigma}(\delta) = 2V_f\tau_s\frac{l_0 - \delta}{r} \tag{1.10}$$

where $\bar{\sigma}$ is the far field stress, V_f - fibre volume fraction.
Fibre pull out work is then expressed from the work integral in which the limits are 0 (no crack opening) and l_0 - fibre completely pulled out of the matrix.

$$W = 2V_f\frac{\tau_s}{r}\int_0^{l_0}(l_0 - \delta)d\delta \tag{1.11}$$

$$W = 2V_f\frac{\tau_s}{r}\int_0^{l_0}\Big[l_0\delta - \frac{\delta^2}{2}\Big]_0^{l_0} \tag{1.12}$$

$$W = V_f \frac{\tau_s {l_0}^2}{r} \tag{1.13}$$

Since pull out fibre length l_0 cannot be longer than critical fibre length l_c (due to stress transfer - fibres surrounded by matrix are loaded by failure stress only if the length is larger than the critical length) as well as substituting terms $\tau_s l_c / r$ for maximal stress in the fibre [8] one gets equation relating fibre volume fraction, ultimate failure stress and interfacial shear stress with the average pull out work per fibre. The numerical term $\frac{1}{12}$ has been found to fit experimental data by Kelly.

$$W = \frac{1}{12} V_f \sigma_f l_c \tag{1.14}$$

As it can be seen from the equation 1.15 the fibre pull-out work and consequently the fracture toughness of the composite is directly proportional to the fibre volume fraction in the composite as well as interfacial shear strength of the interface and fibre diameter as $l_c = \sigma_f d / 2\tau_s$. This in part explains higher glass fibre composites fracture toughness as glass fibres are usually more than twice in diameter compared to carbon fibres.
In fact fibre pull out is reported to be the dominant energy dissipation mechanism for the carbon fibre reinforced plastics while in glass fibres in addition to pull-out mechanism that is more significant than in carbon fibres post-debond sliding is reported to be higher in magnitude [4].

Such energy absorption mechanism that is hugely important for the composite toughness. It has been stated by Lilholt (1994) that the ratio between energies of fibre pull-out and debonding can typically be in the range of 50 to 200. It is determined by the fibre stiffness and ultimate strength [3].

$$\frac{w_l}{w_d} = \frac{E_f}{\sigma_{fu}} = \frac{1}{\epsilon_{fu}} \tag{1.15}$$

1.7. Composites recycling

Sustainability is a very relevant topic nowadays with many initiatives being created to increase the usage of second life materials and decrease the amount of ones that end up in landfills in addition to using materials that easily break down if it gets into the nature (e.g. microplastics floating in the oceans that are not able to break down are a major concern for well being of wildlife as well as humans). In terms of composites, industries such as automotive has been including non-structural bio-composites in the cars they produce. Examples of parts made using bio-composites are shown in figure 1.9 below. Most of the time such parts are not visible and non-structural as on one hand it is difficult and potentially more costly to achieve great surface finish when compared to common plastics for the use of inside cabin panels. On the other hand concern over fracture resistance, less predictable and depending on the natural fibres used - worse mechanical properties and moisture absorption among other things limit bio-composites usability in place of traditional materials such as steel or aluminum for structural applications.

Fig. 1.9 Parts manufactured utilizing bio-composites in Mercedes-Benz vehicle [22]

A shift towards more eco-friendly materials is very much related to the regulation issuing trends. For example in the EU only 5% of the car weight is allowed to be incinerated at its end of life. Meaning all of the 95% has to be recyclable. That is especially concerning for the composites who are inherently difficult to recycle compared to common plastics and metals.
There exists methods to extract fibres from the end-of-life composite, however thermoset matrix cannot be further used for the chemical structure reasons discussed previously. One of such methods is pyrolysis in which the composite is burned with the energy from the burning matrix being used as a heat source and what is left then are the fibres. Such technique can be effectively used for carbon fibres which retain up to 90% of their strength after the operation. However, it is not an effective way of recycling glass fibre composites as glass fibres may lose up to 80% of their strength depending on the glass composition [23] after being treated in a pyrolysis required temperature of 450°C. The other commonly used method is the mechanical grinding. During this method the end-of-life composite parts are first shredded and then grinded into fine powder. It is then separated into resin and fibre parts of which the resin can be used as a filler in applications where that is required. Of course there exist quite a few solutions for recycling and reclaiming the fibres from the thermoset composites even achieving close to 100% of the original mechanical properties [24], however, these methods are not yet developed to be used in high quantities as required by the industries. Thermoplastics, on the other hand, can be very efficiently recycles by the previously discussed mechanical grinding method as both the fibres and the resin can be reused.

2. Impact tests on thin composite panels

In the following chapter a study on the impact properties of the UD carbon/Twill glass fibre prepared with conventional epoxy resin system as well as with novel PMMA resin manufactured by Ottobock is presented. First the PMMA resin mechanical properties are determined and compared to epoxy. Following that specimens are prepared using vacuum assisted hand lay-up. The experiment setup, including the machine introduction, specifications and fixtures are all detailed in this section.

2.1. Material data

The mechanical properties for the epoxy resin are well known and documented. However, in the case of PMMA resin, tensile tests had to be performed as the manufacturer does not provide mechanical material properties for the product. The test specimens (figure 2.1) have been produced according to ASTM D638 standard with cross section of 13x6 mm. At the specimen ends additional rubber pieces are bonded to reduce slippage at the grips. During the tensile tests the extension is measured by extensometers (figure 2.2) which is later recalculated into strain in both longitudinal and transverse directions.

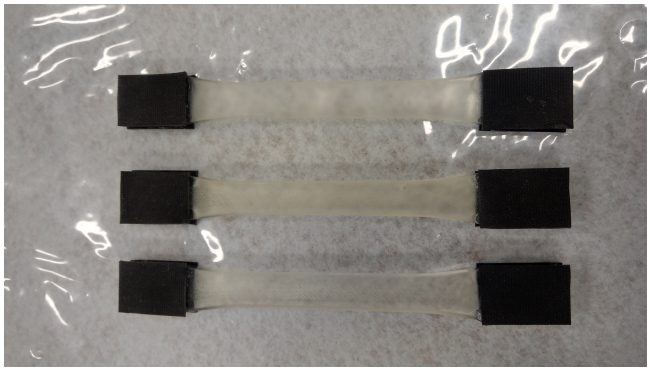

Fig. 2.1 PMMA resin tensile test specimens.

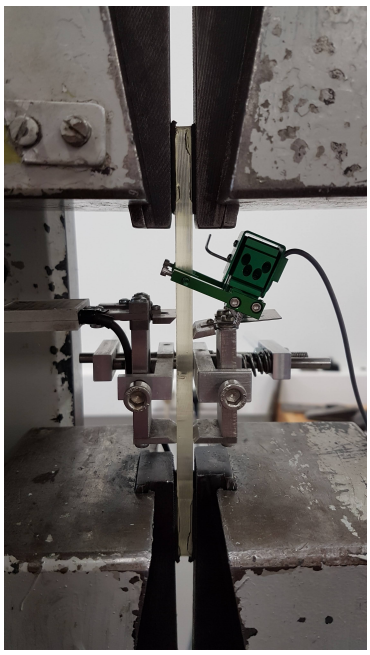

Fig. 2.2 PMMA resin tensile test setup.

Below in figure 2.3 a Stress-Strain graph for the 4 tested specimens is presented. For the ultimate strength and strain property calculations only specimens 3 and 4 are selected as specimens 1 and 2 possibly fractured prematurely due to flaws or other reasons. Also because it is of interest to find out the maximal mechanical capabilities of the resin. Hence the Ultimate Tensile Strength $\sigma_{ult} = 44.3$ MPa with the corresponding failure strain $\epsilon_{fail} = 2.19$ % which would indicate a brittle behaviour which has also been observed during the experiments as no ”necking” has been visible and a sudden failure has occurred. Interestingly the PMMA resin failure strain value has been found to be more than three times lower than that of Epoxy. That is not what is normally expected from common thermoplastic materials. The Ottobock resin, however, is not the usual thermoplastic material and thus the strain values are accepted. Tensile modulus has been calculated from the Stress-Strain data in the $0.05-0.25$ % strain range. The average Tensile modulus from the 4 tested specimens is calculated as $E = 2.45$ GPa. Similarly the Poisson’s ratio is found to be 0.54.

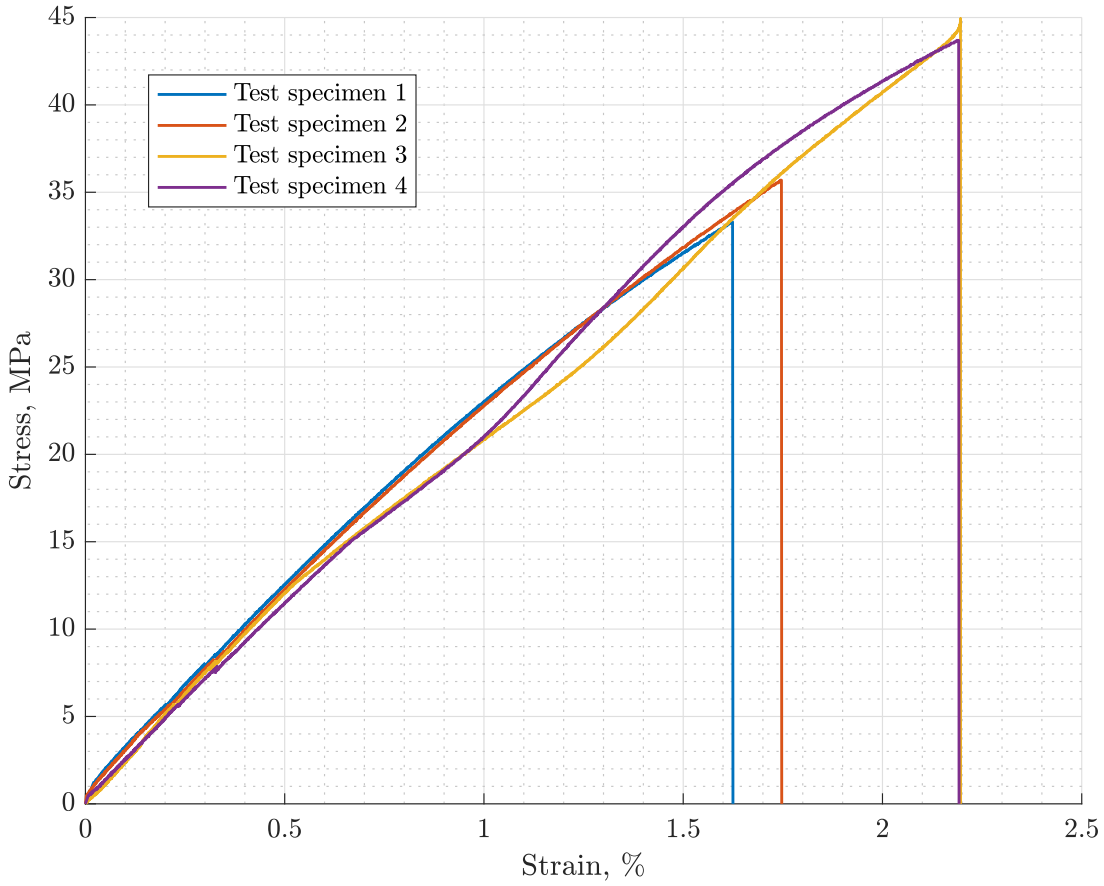

Fig. 2.3 PMMA resin test specimens Stress-Strain graph

The brittle fracture shape is presented in the figure 2.4 below. It can clearly be seen that there is break characteristic to brittle materials with no apparent necking near the fracture and two even fracture surfaces.

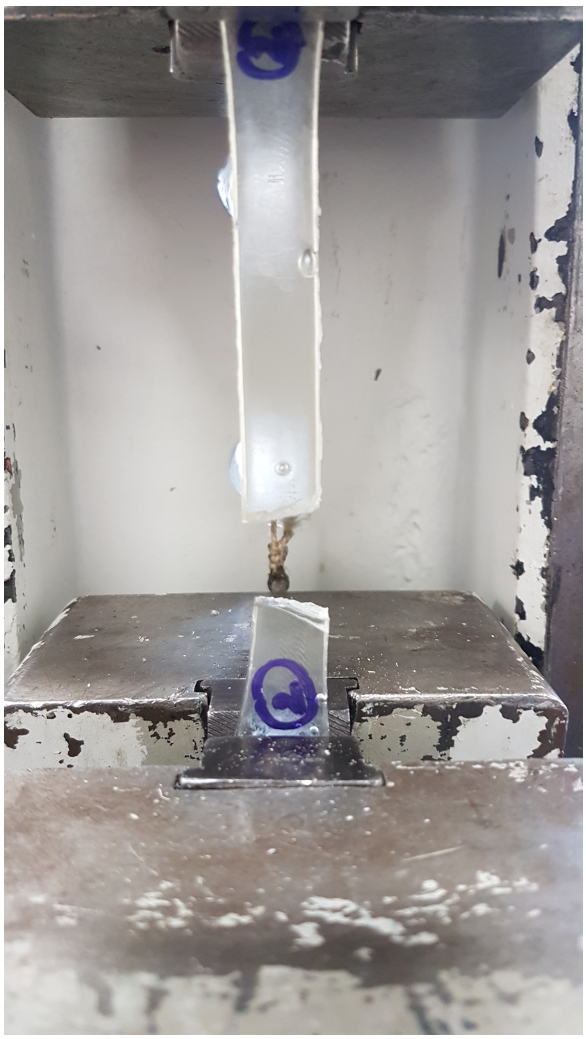

Fig. 2.4 PMMA resin test specimen fracture shape

Table 2.1 PMMA (Ottobock 617H19).

Parameter	**Specification**
Tensile modulus (GPa)	2.45
Ultimate strength (MPa)	44.3
Strain at failure (%)	2.19
Poisson's ratio	0.54

Table 2.2 Biresin CR83.

Parameter	**Specification**
Tensile modulus (GPa)	2.96
Ultimate strength (MPa)	84
Strain at failure(%)	6.7
Poisson's ratio	-

The calculated tensile modulus of the Ottobock PMMA resin is comparable to that of CR83 epoxy resin, however, the Ultimate strength and Strain at failure are significantly lower which indicates that at least at room temperature the PMMA resin is significantly more brittle than the epoxy resin.

Table 2.3 Uni-directional carbon fibre material properties

Parameter	**Specification**
Tensile modulus (GPa)	55
Ultimate strength (MPa)	2200
Strain at failure(%)	0.8
Poisson's ratio	0.2

2.2. Experiments setup

The impact experiments on composite panels in various configurations are performed on the high-speed impact testing machine Magnus 1000 manufactured by Coesfeld. Main characteristics of the test machine are as follows:

Table 2.4 Technical specifications of high speed impact tester Coesfeld Magnus 1000

Parameter	**Specification**
Impact speed	up to 42 m/s
Impact energy	up to 4.5 kJ
Temperature chamber	-50...150 °C
Impactor (sphere)	d = 10/15/20 mm
Specimen shape	50...200 mm

The parameters for the tests are:

- Impactor weight - 5.185kg
- Impactor tip radius - 20mm
- Impact velocity - 7m/s

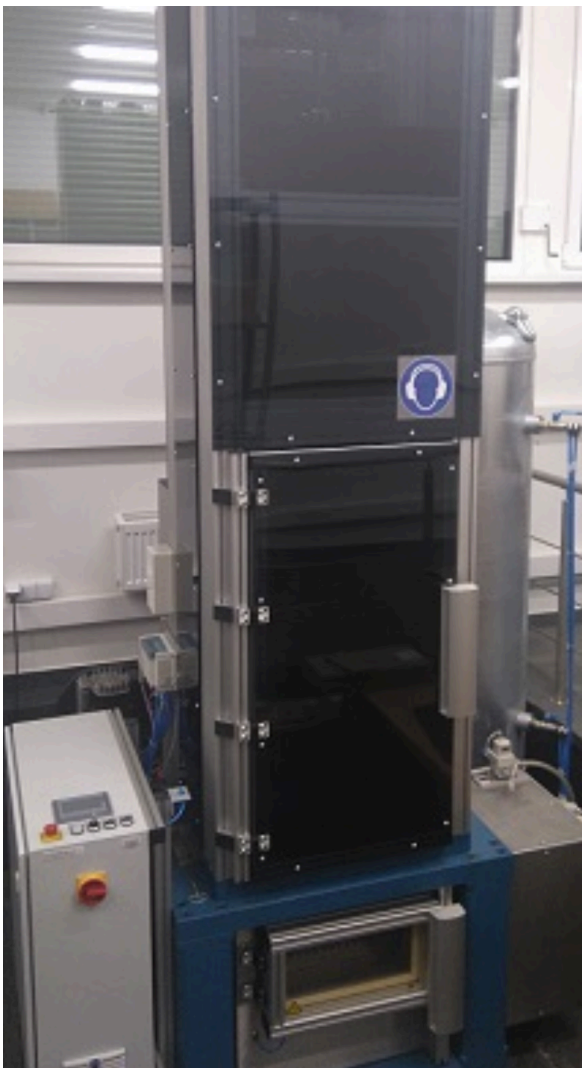

Fig. 2.5 Impact testing machine Magnus 1000 at the mechanical testing laboratory of Kaunas University of Technology

The specimen is clamped inside the testing chamber by steel clamps as can bee seen in the figure 2.6. The panel is positioned on top of the fixture by hand and is clamped automatically after the chamber is closed. The testing machine has the capability to cool or heat the specimens in the tempering chamber. The accuracy for the setting of the temperature is $\pm 0.1^{\circ}$C and control accuracy of $\pm 1^{\circ}$C. The temperature is increased or decreased gradually, keeping the chamber temperature higher than the sample temperature by approx. 10°C until target is achieved.

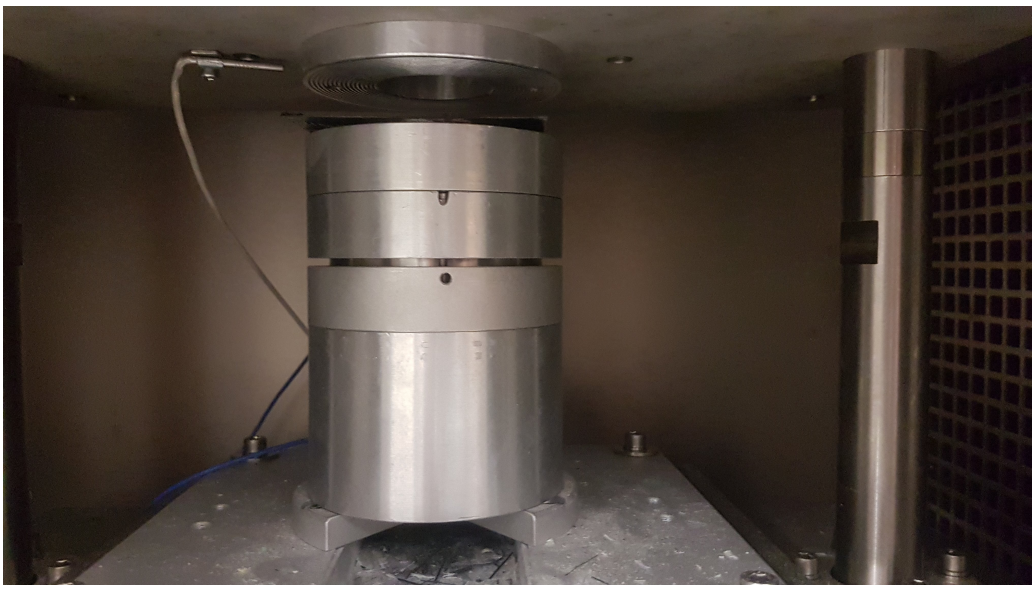

Fig. 2.6 Impact test specimen fixtures inside the tempering chamber.

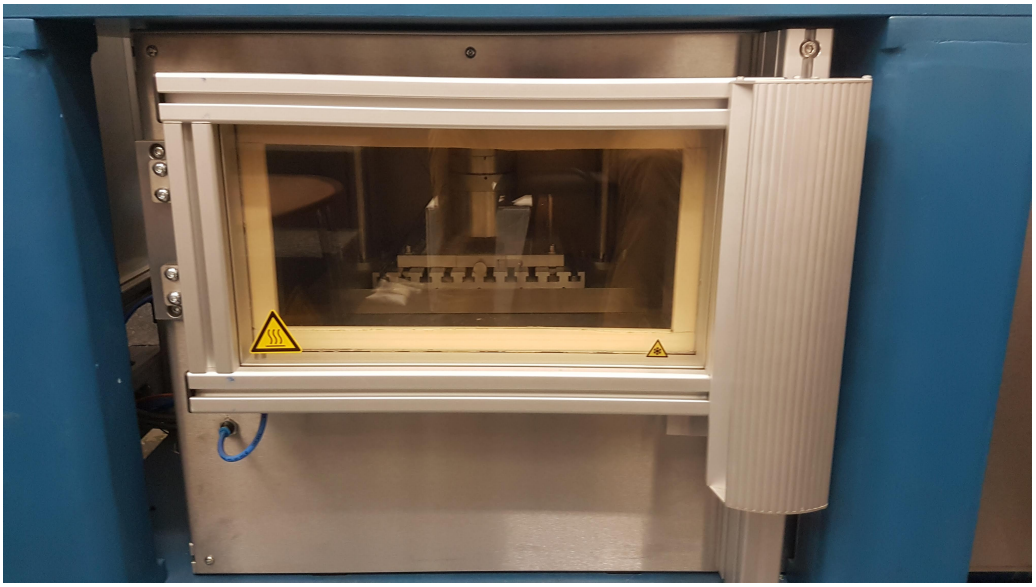

Fig. 2.7 Tempering chamber view from the outside.

2.3. Test specimen preparation

The composite panels are prepared with 4 layers of carbon fibre UD fibre cloth in a symmetric configuration - [0/90/90/0] (figure 2.12) or in the case of glass fibre which is in twill configuration - simply stacked 4 layers identically to one another.

The panels are produced by hand laying them and spreading the resin on each layer until it can be visually seen that there are no dry fabric spots (2.8).

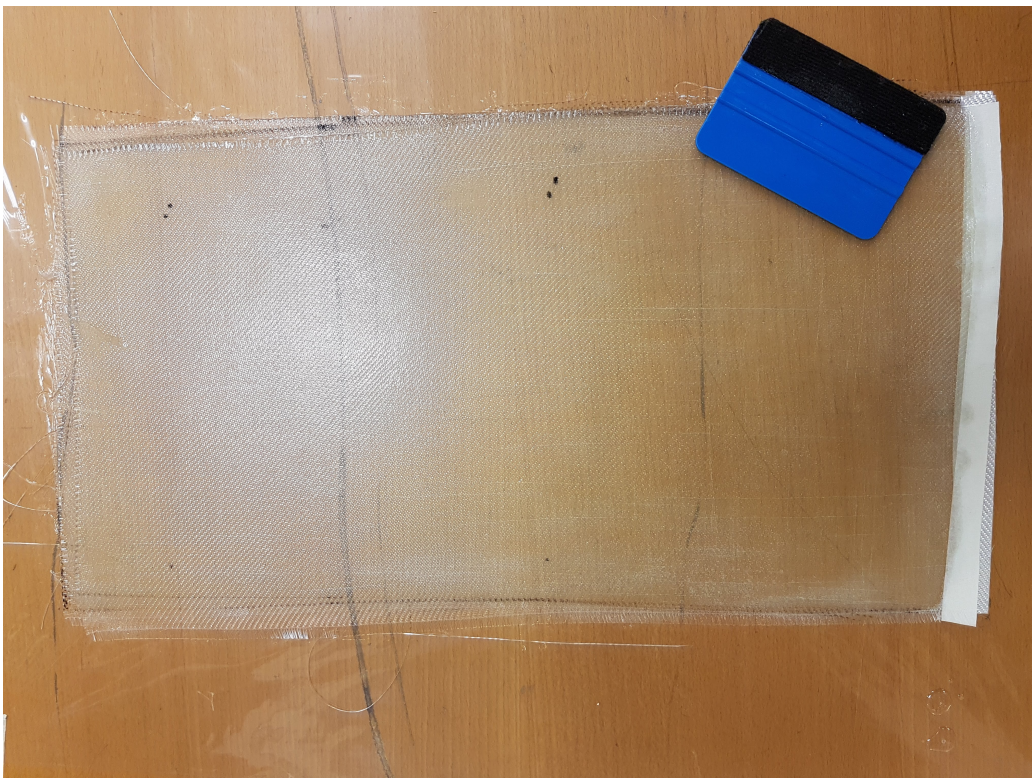

Fig. 2.8 Panels hand-layup and resin infusion

Non-stick fabric (figure 2.9) is placed on top of the resin-wetted glass or carbon fibre plies. It is carefully placed so that no wrinkles are present. On top of it a felt fabric (figure 2.10) is placed which serves a function of soaking the excess resin during vacuuming process.

Fig. 2.9 Non-stick fabric used for panel production

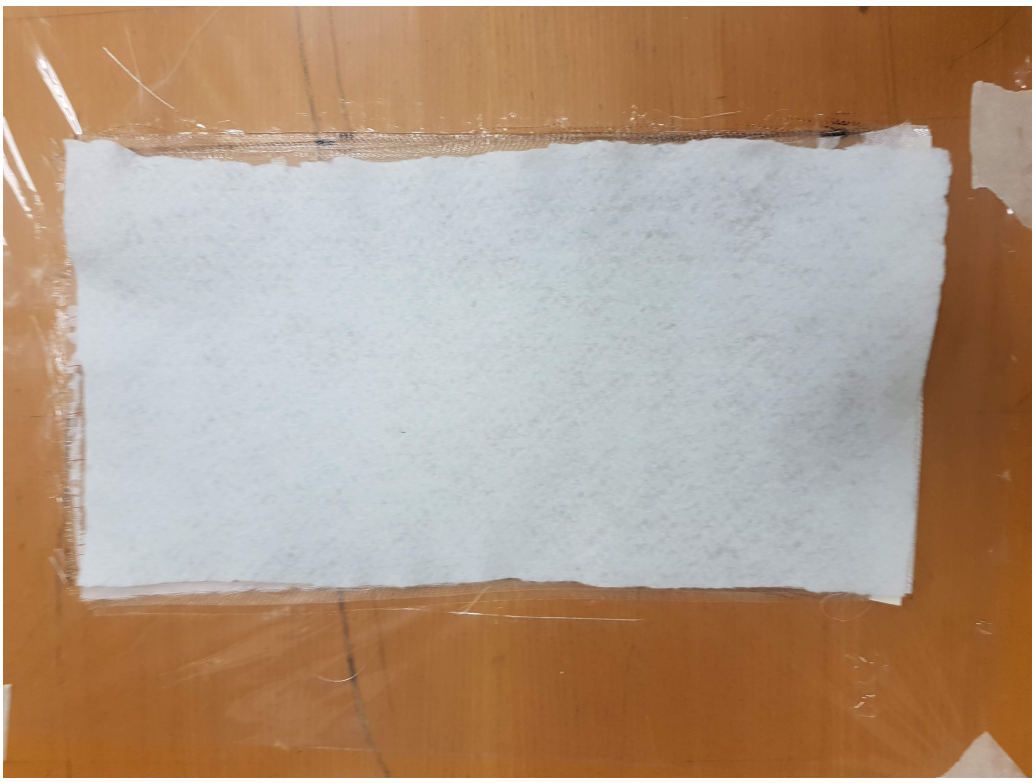

Fig. 2.10 Fabric used to soak in extra-resin during consolidation

The last step is sealing an area around the panels with plastic film and creating a vacuum which minimizes the porosity in the panels as they consolidate (figure 2.11).

Fig. 2.11 Vacuum setup

Samples are then cut to size of $70x70$mm which is just large enough to provide enough gripping surface for the clamp in the testing machine.

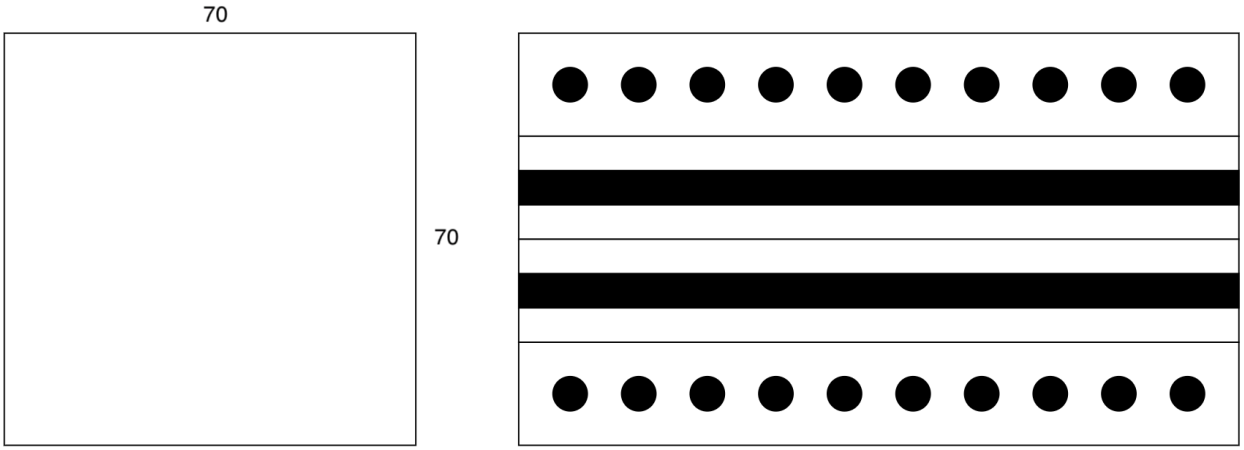

Fig. 2.12 Test specimen configuration

3. Results discussion

The novel PMMA resin by Ottobock is compared to conventional resin system - in this case epoxy. Temperature effects are investigated during impact tests on thin specimens made with carbon fibre plies.

3.1. UD carbon fibre specimens

In the following chapter results of the impact tests for the carbon/PMMA resin are presented and compared with conventional carbon/epoxy specimens. In the tables 3.1 and 3.2 several characteristic values are presented: F_m - Maximum impact force (kN) absorbed by the test specimen; F_d - Force (kN) measured at the point where damage has been first initiated in the test specimen; E_m - Energy (J) absorbed up to the point where maximum force has been recorded; I_d - Deformation (mm) at the moment when damage has been first initiated.

Table 3.1 PMMA/carbon specimen data

No.	Temp.	F_m	F_d	E_m	I_d
	°C	kN	kN	J	mm
1	14	1.98	1.76	4.71	2.85
2	14	2.13	1.16	3.15	2.53
3	14	1.65	0.55	5.90	2.13
4	14	1.58	1.46	4.11	2.94
5	39	1.76	0.67	3.91	1.43
6	40	1.55	1.10	1.96	2.28
7	37	1.48	0.84	4.66	1.38
8	61	1.49	0.70	2.19	1.27
9	60	1.76	0.80	2.39	1.57
10	60	2.05	1.55	5.19	2.97
11	60	1.65	1.12	5.42	2.59
12	60	1.67	0.90	4.13	2.34
13	81	1.80	1.80	2.73	3.58
14	81	1.84	1.82	5.60	3.65
15	82	1.79	0.79	3.80	2.48
16	80	2.04	1.31	2.88	2.74

Table 3.2 Epoxy/carbon specimen data

No.	Temp.	F_m	F_d	E_m	I_d
	°C	N	N	J	mm
1	13	2.56	1.42	7.23	2.07
2	13	1.2	0.77	3.78	3.19
3	41	1.42	1.42	2.23	4.14
4	41	2	0.95	3.12	2.35
5	62	3.77	2.39	10.70	4.23
6	63	3.71	3.58	10.20	6.16
7	81	4.34	3.14	11.52	4.22
8	83	2.92	2.47	6.09	3.65

It can be observed from the figure 3.1 below that the Carbon/PMMA specimen temperature

has little to no effect on the maximum impact force that the specimen is able to withstand. The Carbon/epoxy specimens, however, perform better with increased temperature. It is interesting to observe that both specimen types perform similarly in the 13°C and 41°C temperature range. Even though at these temperatures, the PMMA samples have significant amount of debonding, especially at the bottom layer while the epoxy samples have barely any. This could indicate better adhesion between carbon and epoxy than that of PMMA and carbon at low temperatures. Through-crack being more favourable path from energy release rate standpoint against delamination/debonding for the epoxy composites. Also it has been observed that at approx. 40°C both resins perform worse than at room temperature while recovering at higher temperatures. At temperatures higher than 80°C the epoxy is clearly superior reaching $F_{max} = 4.34$ kN which is more than double than $F_{max} = 2.045$ kN of PMMA. There is relatively high spread of data points for the epoxy specimens which could be attributed to the inconsistencies and flaws in the specimens and the fibres themselves. However, the maximal points are the most important as they indicate the state of the materials system that has been manufactured to be closest to ideal as possible.

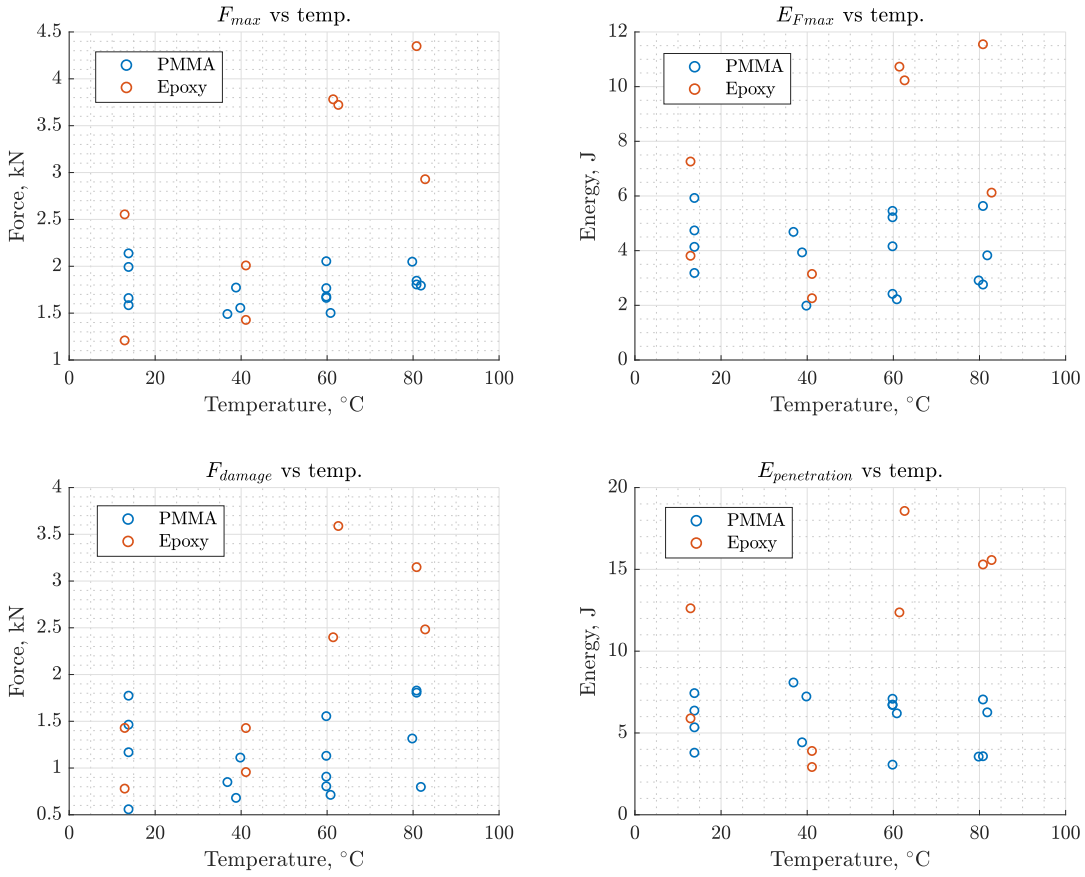

Fig. 3.1 F_{max}, F_{damage}, E_{Fmax} and $E_{penetration}$ dependency on the temperature for Carbon/PMMA and Carbon/Epoxy composites

In the figures 3.2 and 3.3 the samples at corresponding test temperatures for both epoxy and PMMA are presented. While for the specimens made with epoxy resin, the failure mechanisms are largely

the same at any temperature, for the PMMA some differences can be observed. At room temperature some energy is dissipated by the both intra-layer and inter-layer debonding as evident by the impact shapes for the RT and $40°C$ specimens. For the $60°C$ specimen there are very few debonded or delaminated groups of fibres and at $80°C$ a clean diamond-shaped fracture occurs similar to those of epoxy specimens. The reason for this behaviour could be the increase in temperature strengthens the adhesion between the resin and fibre phases which makes debonding and delamination less favourable for crack propagation. However, the energy consumed by crack debonding and delaminating the plies is not significantly high at those low temperatures as evident by the absorbed energy remaining fairly constant throughout the different testing temperatures at $1.958 - 5.897J$ presented in the figure 3.1.

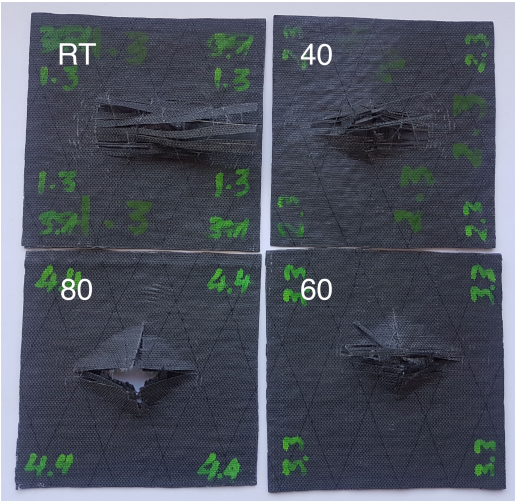

Fig. 3.2 Carbon/PMMA specimens.

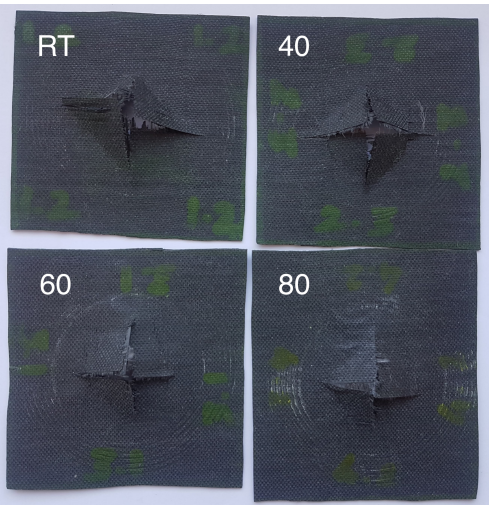

Fig. 3.3 Carbon/epoxy specimens.

The differences between Carbon/PMMA and Carbon/Epoxy composites are further detailed in the figure 3.6. The ripples in the F-displacement graphs of the PMMA specimens are indicative of severe delamination/debonding, whereas epoxy specimens display more of a sudden failure with barely any recovery after damage has been initiated as is illustrated by the rapid drop in force. Most importantly, the PMMA resin show similar mechanical characteristics at low temperatures ($13 - 40°C$) but does not match epoxy at higher ($60 - 80°C$) temperatures. The difference could be partially influenced by the composition of the PMMA resin related to plasticity at increased temperatures - from the tables 3.1 and 3.2 it can be seen that at higher temperatures the damage is initiated at higher displacement for the epoxy/carbon composites compared to PMMA/carbon ones.

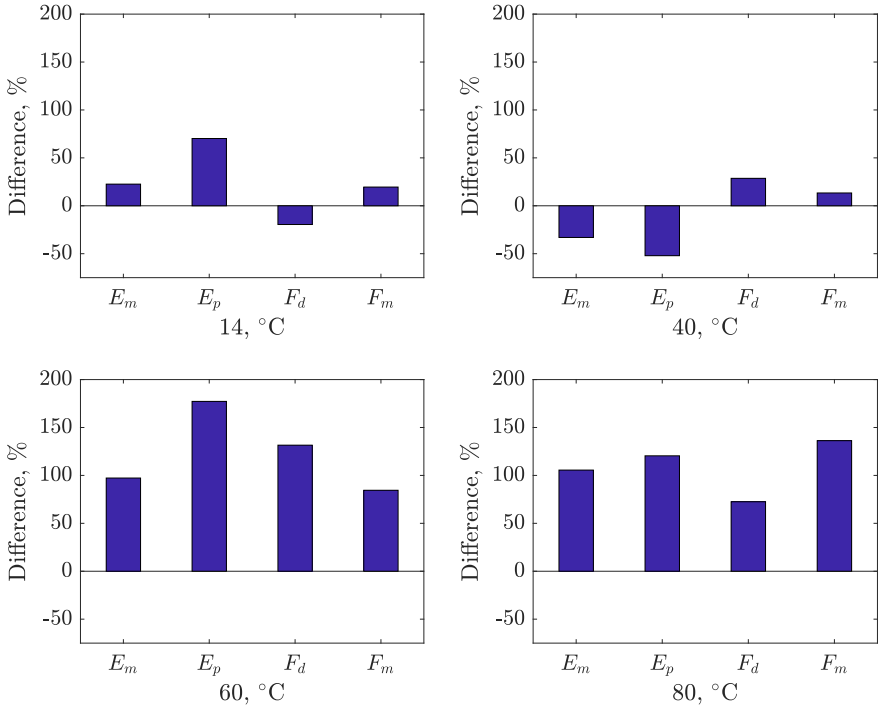

Fig. 3.4 Percentage difference between carbon/epoxy and carbon/PMMA composites impact resistance parameters(comparing maximum values at each temperature).

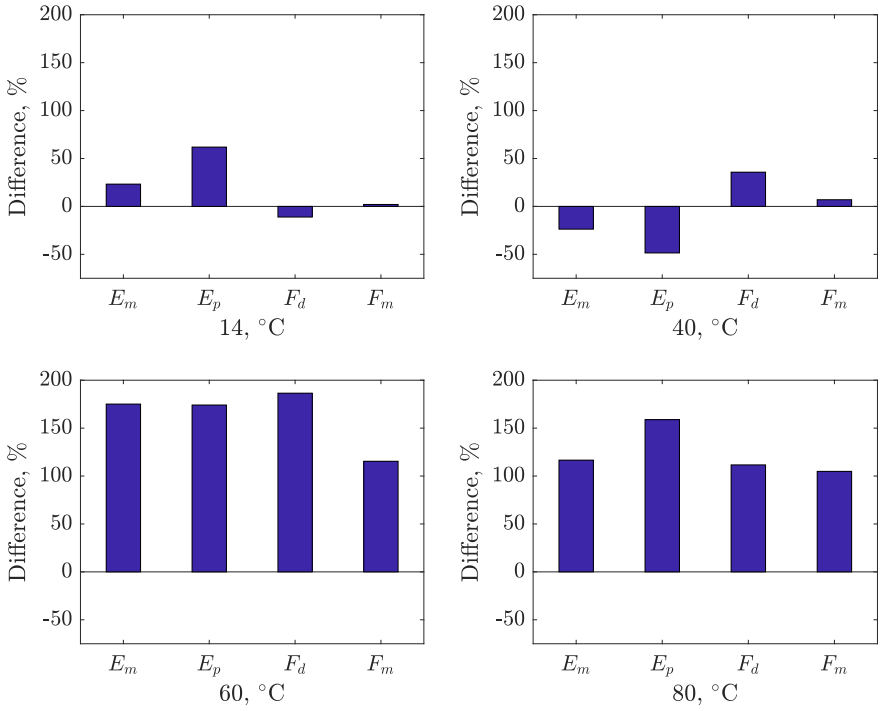

Fig. 3.5 Percentage difference between carbon/epoxy and carbon/PMMA composites impact resistance parameters(comparing maximum values at each temperature).

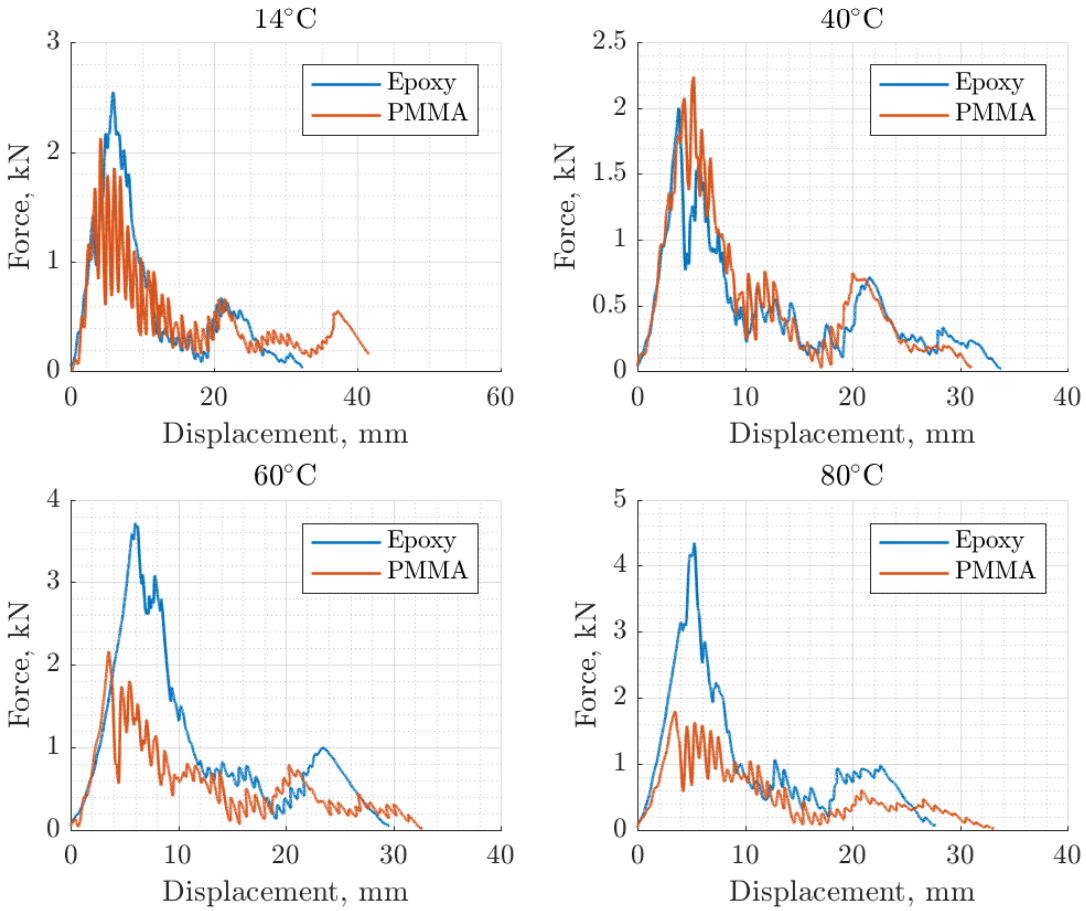

Fig. 3.6 Force-Displacement graphs for 4-layer (0/90)s carbon-epoxy and carbon-PMMA laminates at different temperatures.

3.2. Twill glass fibre specimens

Identically to the carbon fibre specimens, the twill glass fibre specimens are tested at four different temperatures - Room Temperature(16)°C, 40°C, 60°C and 80°C. The dimensions and the thickness are kept the same ($70x70$mm and 1mm respectively). Thus the only difference being the twill glass fibre plies being used.

The fabrication of the twill glass fibre specimens proved to be significantly more difficult when using Ottobock PMMA resin when compared to epoxy resin. This can be attributed mainly to higher viscosity which makes impregnation slower as well as shorter setting time. The setting time is stated to be 60 minutes by the manufacturer has been found to be accurate, although when using hardener in a ratio of $2:100$ the setting time is then 80 minutes which gives more time to properly spread and impregnate the fibre plies.In the last part of the hardening an exothermic reaction can be observed.

Below in the figures 3.7 - 3.19 the test specimens are presented at each of the four temperatures from the top and bottom sides.

Table 3.3 Epoxy/glass specimen data

No.	Temp.	F_m	F_d	E_m	I_d
	°C	kN	kN	J	mm
1	16	3.81	3.287	7.746	3.82
2	16	4.77	3.98	11.15	4.41
3	16	3.66	3.13	5.70	3.52
4	44	5.65	5.65	12.25	5.60
5	43	5.90	5.90	12.35	5.1
6	43	4.62	4.62	8.83	5.21
7	63	5.42	5.42	11.44	5.11
8	65	5.89	5.89	11.97	5.28
9	91	5.83	5.83	16.81	6.02
10	86	6.07	6.07	18.84	7.63

Table 3.4 PMMA/glass specimen data

No.	Temp.	F_m	F_d	E_m	I_d
	°C	kN	kN	J	mm
1	16	3.63	3.06	7.99	3.92
2	16	3.78	3.40	7.44	3.88
3	16	4.58	4.58	8.19	4.50
4	46	4.24	7.36	7.36	4.44
5	46	2.98	5.73	5.73	5.18
6	47	3.21	5.3	5.34	4.99
7	67	4.16	4.16	8.19	4.94
8	65	4.41	4.41	6.47	3.85
9	89	7.39	7.39	11.47	4.51
10	87	5.25	5.25	9.80	5.19

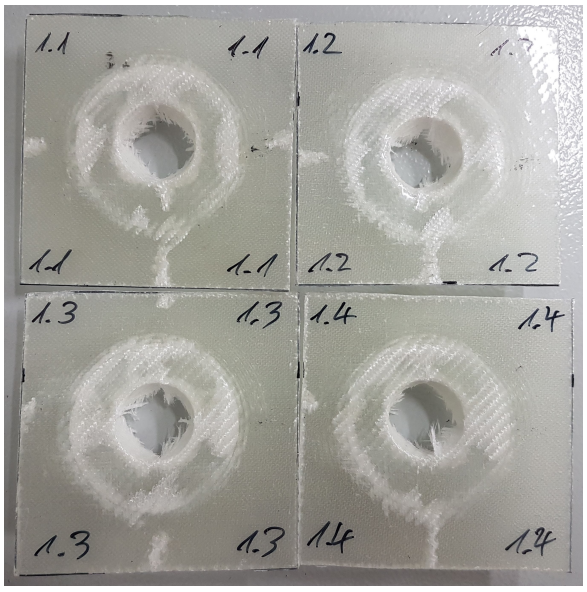

Fig. 3.7 Glass/epoxy samples(RT) - top

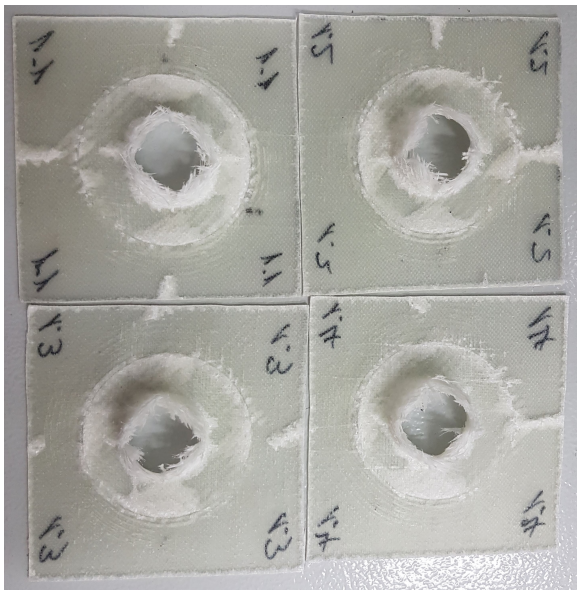

Fig. 3.8 Glass/epoxy samples(RT) - bot

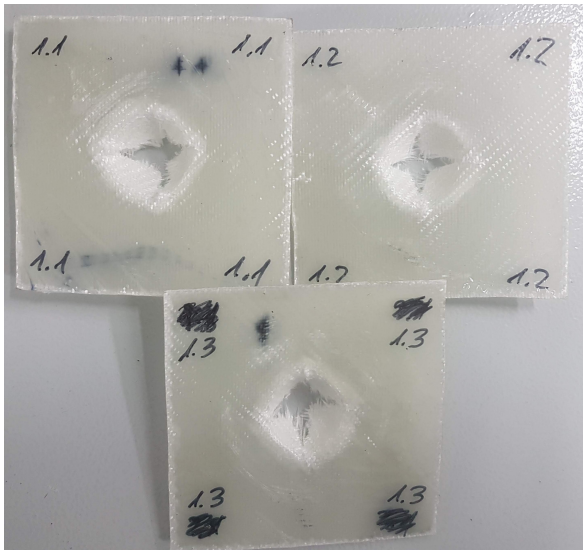

Fig. 3.9 Glass/PMMA samples(RT) - top

Fig. 3.10 Glass/PMMA samples(RT) - bot

Differently from the UD carbon fibre specimens, at room temperature the impact area looks rather uniform both across the impact hole diameter and in terms of differences between the samples. There are fewer delaminaitons as one would expect from twill weave plies. Severe delaminations have been an issue when using UD plies and so it could be expected the with more intricate geometries(i.e. twill weave) PMMA resin type with longer setting time should be used. UD laminates are more susceptible to flaws and when crack propagates such weak spots quickly turn into failure spots. For the twill weave laminates, on the other hand, suppress crack growth by the mechanism of prohibiting inter-laminar delamination which leads to increased puncture resistance.

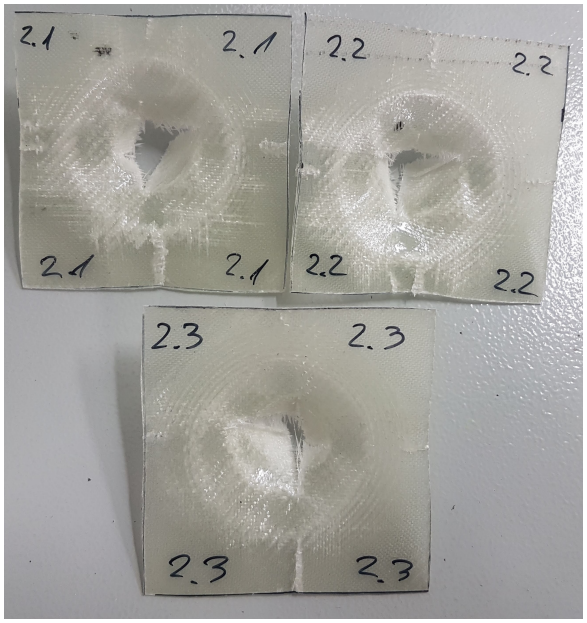

Fig. 3.11 Glass/epoxy samples(40°C) - top

Fig. 3.12 Glass/epoxy samples(40°C) - bot

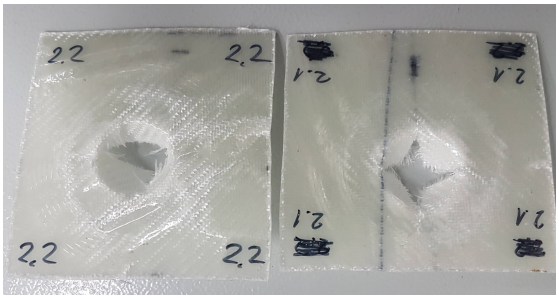

Fig. 3.13 Glass/PMMA samples(40°C) - top

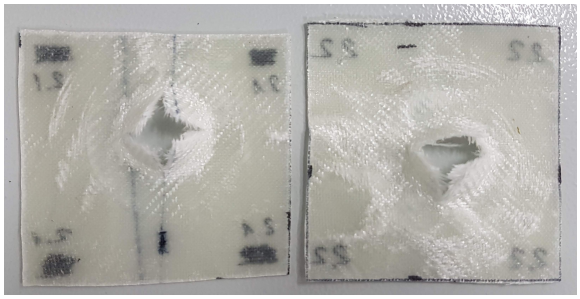

Fig. 3.14 Glass/PMMA samples(40°C) - bot

As the temperatures are increased, the specimens become more plastic as evident by the larger damaged area (white delamination spots) and buckling at the edges for both epoxy and PMMA. Moreover, the hole being punched by the impactor is increasingly less defined for higher temperatures as more energy is being absorbed by plastic deformation of the whole panel itself. This is especially true for the epoxy specimens.

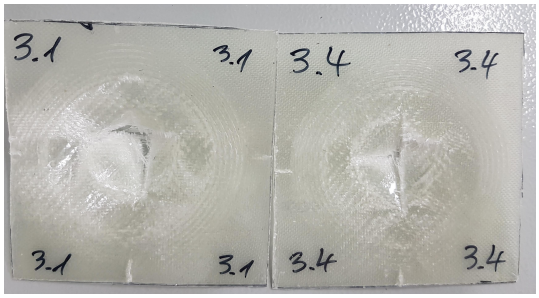

Fig. 3.15 Glass/epoxy samples(60°) - top

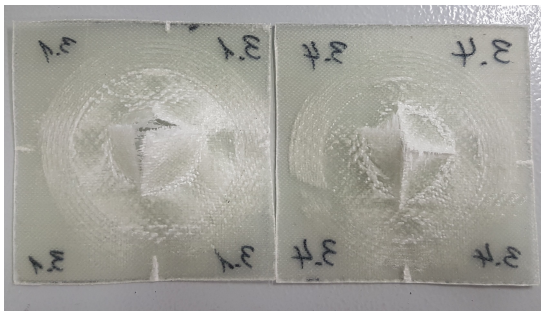

Fig. 3.16 Glass/epoxy samples(60°) - bot

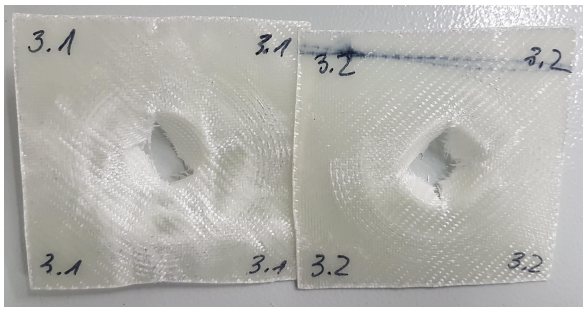

Fig. 3.17 Glass/PMMA samples(60°C) - top

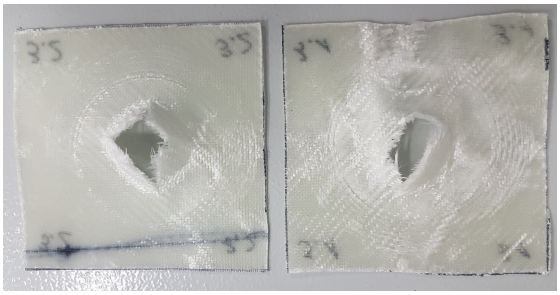

Fig. 3.18 Glass/PMMA samples(60°C) - bot

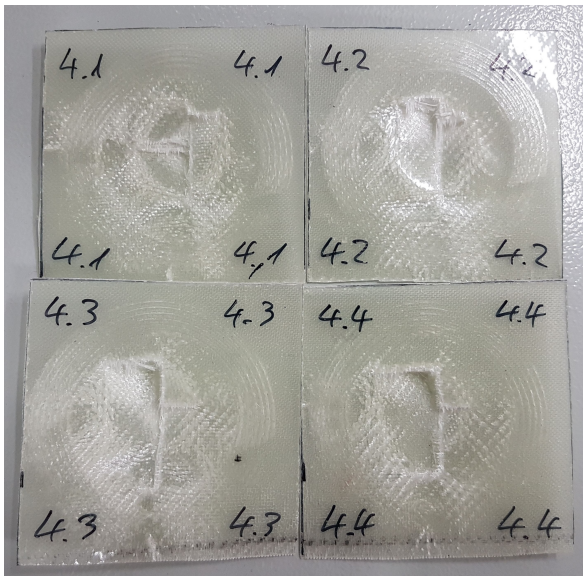

Fig. 3.19 Glass/epoxy samples(80°C) - top

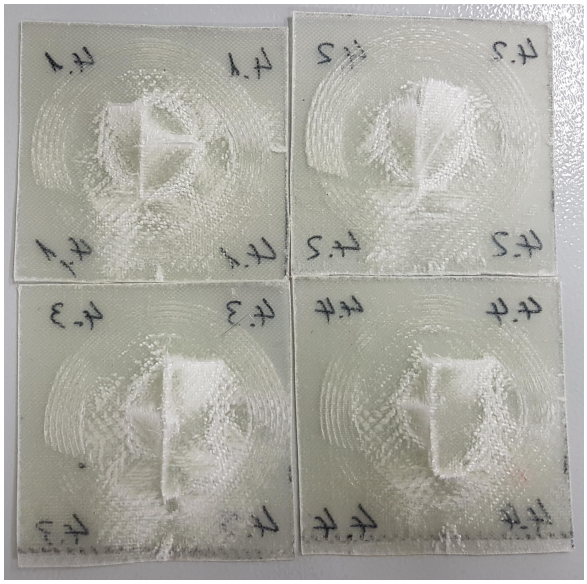

Fig. 3.20 Glass/epoxy samples(80°C) - bot

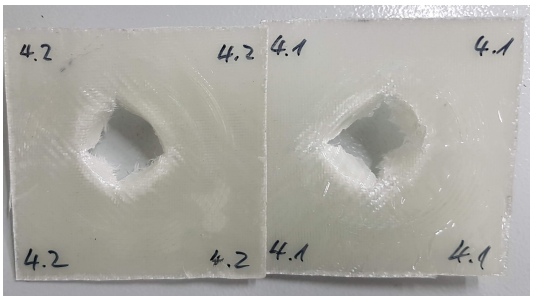

Fig. 3.21 Glass/PMMA samples(80°C) - top

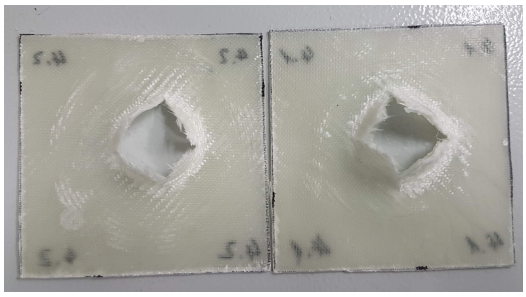

Fig. 3.22 Glass/PMMA samples(80°C) - bot

Below in the figure 3.23 and 3.26 comparisons between epoxy and PMMA test specimens data points are presented. The F_{max} as measured displays an increasing trend with higher temperatures. Epoxy resin laminates consistently across the temperature range absorb higher impact force when compered to PMMA/glass fibre specimens. As seen from the results the F_{max} ranges at $3.66 - 6.07$kN for epoxy and $3.63 - 7.39$kN for PMMA. The percentage-wise difference between these two systems is presented in the figures 3.24 and 3.24 (comparison between mean and maximum values respectively). The epoxy resin in fact performs nearly identical as PMMA at room temperature and $80+$°C but better at intermediate temperatures by a margin of up to 55%. It could be attributed to higher failure strain for epoxy as with higher temperatures induced thermal strains will have proportionally bigger effect for the PMMA resin. At 80°C, however the resins become so plastic so that they have little effect on the impact properties. Consequently the force at which the damage is initiated F_{damage} follows the same pattern where both resins are very much comparable at room temperature with epoxy resin having slight edge at 60°C. Overall in terms of damage initiation force both systems behave with a tendency to increase with elevated temperatures as evident by the data points distribution in 3.23.

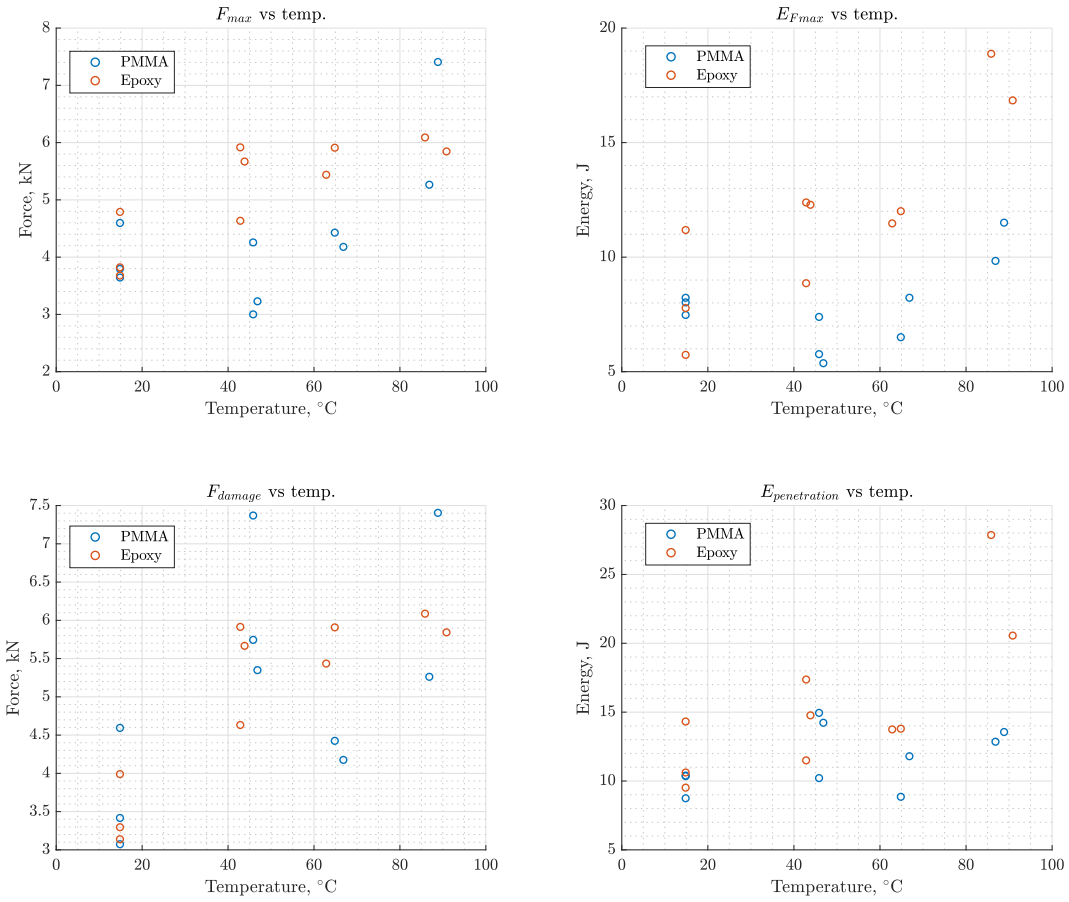

Fig. 3.23 Glass/epoxy specimens data points compared to glass/PMMA specimens data points.

The energy at $Fmax$ is comparable between both resin systems only at room temperature levels. As can be seen from the figures, the tendency is for the absorbed energy at maximum recorded force to increase with elevated temperatures. The maximum value of E_{Fmax} has been measured for PMMA/glass fibre specimens at 89°C of 11.47J which is lower than that of epoxy/glass at the same temperature(18.84J). At 80°, the absorbed energy is significantly higher than at room temperature, with the increase of 330% and 154% for epoxy and PMMA respectively. Such increase could be attributed to the increased plasticity of the specimens as can be seen in the figure 3.26 (a bigger displacement before damage initiation). Essentially the composite panels are more compliant at higher temperatures and thus are able to deform more before reaching their failure strain levels. The PMMA however is more brittle at room temperature by a factor of 3 such difference is expected to remain at elevated temperatures and thus could explain why epoxy absorbs more energy. This is further detailed by the percentage differences between PMMA and epoxy which ranged from 30 to 80% across the tested temperature range. On the other hand, the PMMA deforms less across the temperature range as indicated by the I_d parameter which might be beneficial in some applications. As for the $E_{penetration}$ parameter which also in a way describes the compliance and the plasticity of the laminate, it can be seen that PMMA remains fairly constant at different temperatures with a 43% difference between the

lowest and highest observed values. The epoxy show greater variation of 294% hugely influenced by the high absorbed energy values at 90°C.

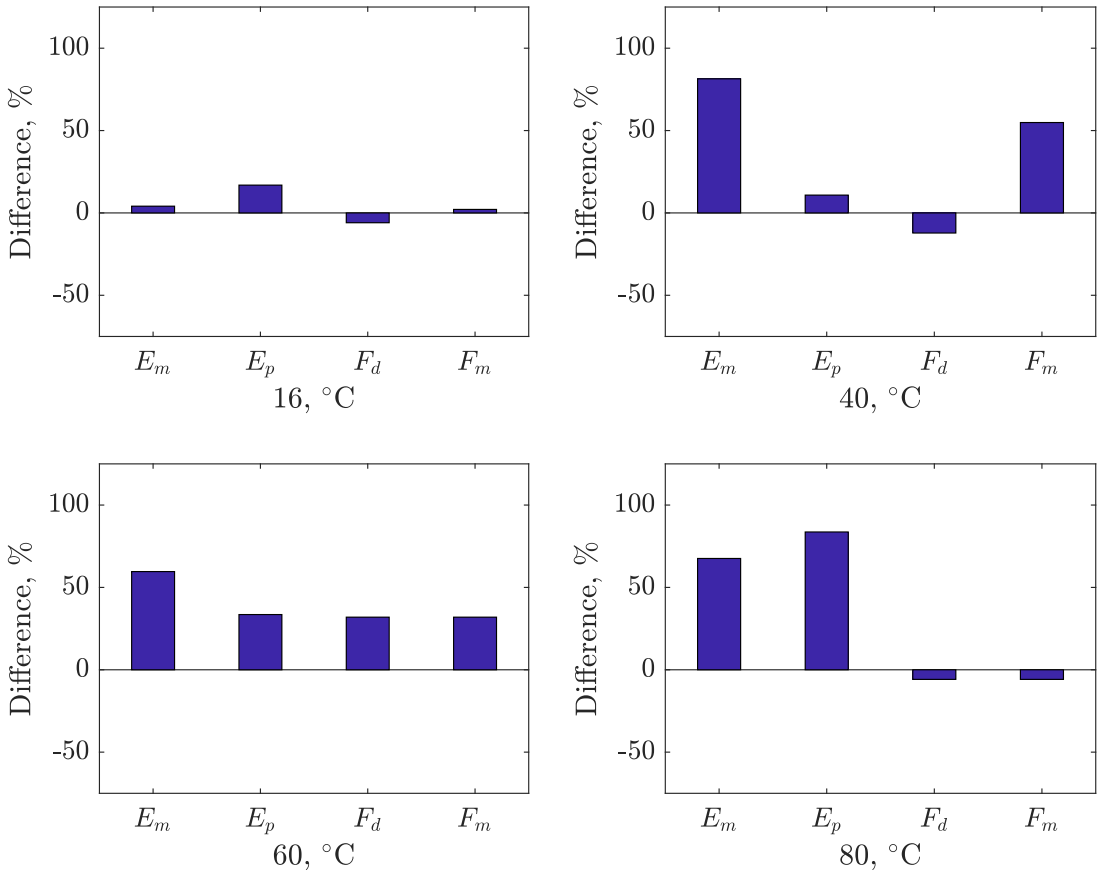

Fig. 3.24 Percentage difference between glass/epoxy and glass/PMMA composites impact resistance parameters(comparing mean values at each temperature).

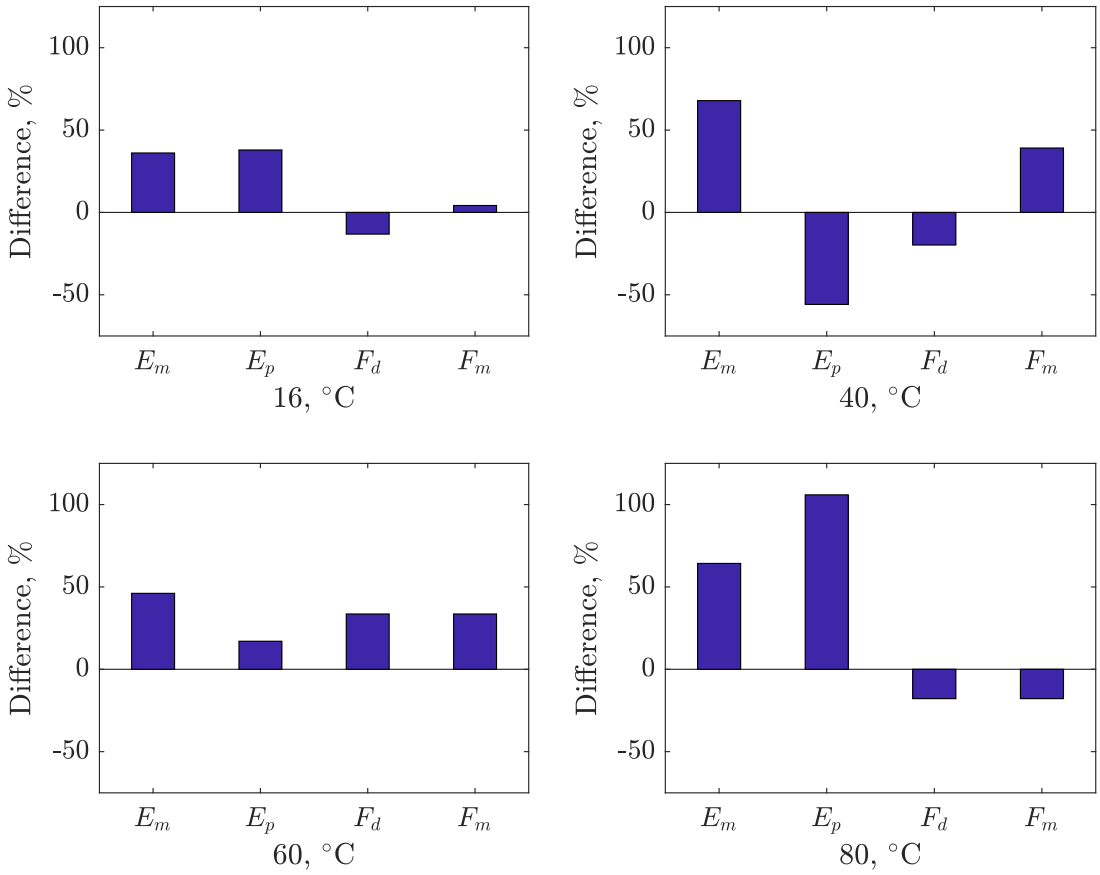

Fig. 3.25 Percentage difference between glass/epoxy and glass/PMMA composites impact resistance parameters(comparing maximum values at each temperature).

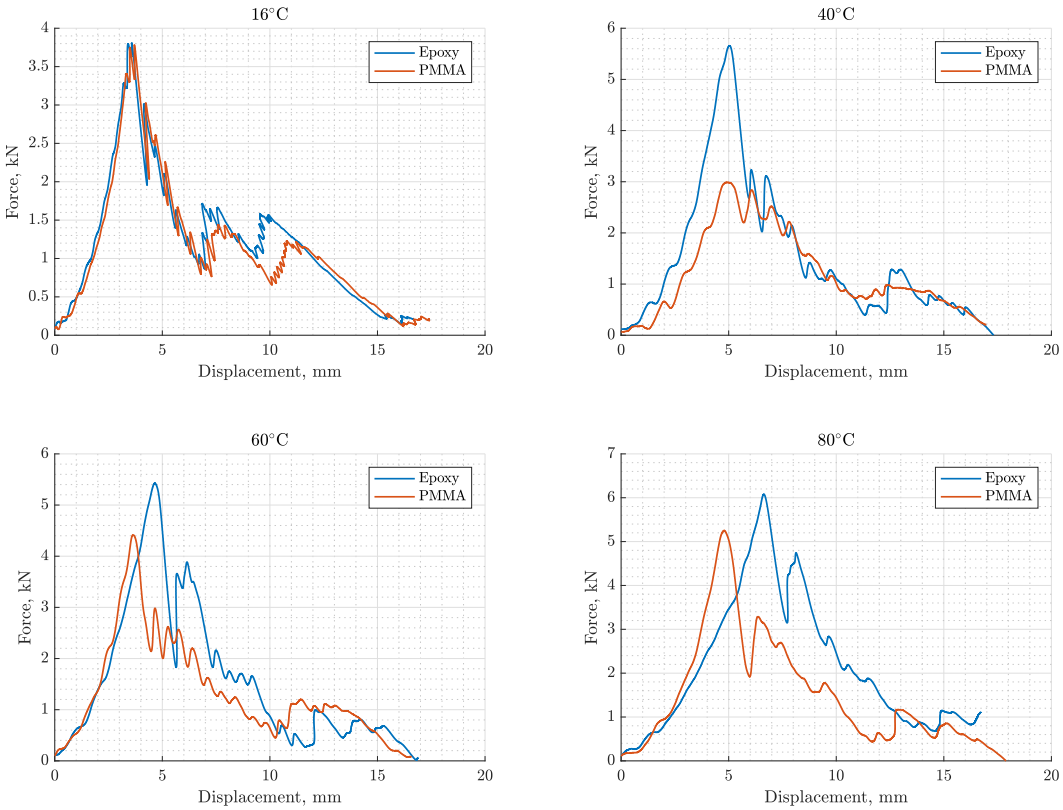

Fig. 3.26 Force-displacement graphs comparison between glass/epoxy and glass/PMMA specimens.

4. Analytic solution

Analytic calculations for maximum deflection can be made following solution by Timoshenko [25]. It does not ideally represent the situation analyzed in this paper as the solution by Timoshenko has a concentrated load in the centre of the plate which is correct at the initial stages of the deformation as the impactor with the 20mm diameter hits the plate. As the deformation continues more and more point come into contact and thus load is then more accurately represented by distributed rather than a line load. Nevertheless, a fairly accurate estimation can be achieve as will be seen by the comparison between calculations and experiments. First, flexural rigidity is calculated:

$$D = \frac{Eh^3}{12(1-\nu^2)} \tag{4.1}$$

Where $h = 1$mm is the thickness of the specimens and E is the tensile modulus which for carbon fibre composite is approx. $100GPa$ ($V_f = 50\%$), $\nu = 0.34$ - Poisson ratio of the composite.
$D = \frac{100 \cdot 10^9 0.001^3}{12(1-.34^2)} = 9.988\text{Pa} \cdot \text{m}^3$. The maximum deflection at the middle of the plate is then calculated by equation:

$$w = \frac{P}{16\pi D}\left[\frac{3+\nu}{1+\nu}(a^2 - r^2) + 2r^2 log\frac{r}{a}\right] \tag{4.2}$$

Where $a = 0.035$m is the diameter of the plate, $r = 0.000001$m is the distance from the centre of the plate. Since the maximum deflections are of interest a very small distance is selected(with $a = 0$ logarithm goes to infinity). P is the applied concentrated load at the plate centre.
Inserting the values one gets the following graph:

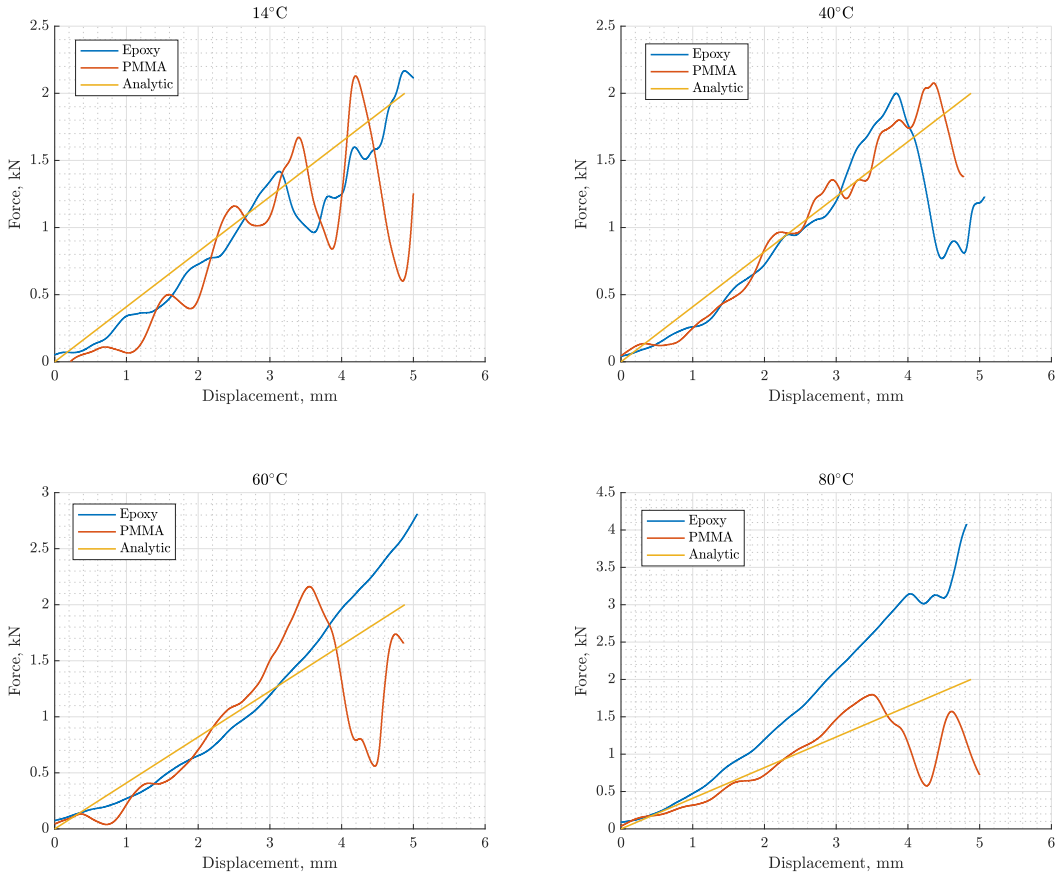

Fig. 4.1 UD carbon fibre (PMMA/epoxy) specimens force-displacement graphs comparison to analytic solution.

The figure 4.1 represents the force displacement curves for carbon/PMMA and carbon/epoxy laminates and their comparison with analytically acquired curve. It can be seen that even at low displacement and force values the experimental graphs are not linear - rather ”ripples” are present which indicate loss of stiffness. Such ”ripples” have higher amplitude for PMMA specimens when compared to epoxy ones. This is expected from previous analysis - It has been observed that novel PMMA resin by Ottobock has worse adhesion properties which results in multiple debonding fractures which can be clearly seen in the figures especially at room temperature. At higher temperatures the adhesion is enhanced and this results in straighter lines - i.e. less debonding due to higher interface fracture energy and thus more energy is stored elastically in the fibres. It is interesting to note that at temperatures above 60°C both PMMA and Epoxy specimens diverge form the analytic solution and showing behaviour of increasing stiffness. This could be attributed to dramatically changing shape of the plate due to elevated temperature.

Conclusions

1) Novel PMMA thermoplastic is suitable to be manufactured using common thermoset methods with curing times of $0.5 - 1.5$h depending on the hardener to resin ratio.
2) Higher PMMA viscosity results in lower fibre volume fraction (by 5-10% compared to epoxy) achieved, especially with more complex geometries (twill weave fibre plies).
3) The impact properties for UD carbon specimens are comparable at temperatures up to $45°$C – $F_{max,epoxy} = 2.56$kN, $F_{max,PMMA} = 2.13$kN while at temperatures $> 60°$C PMMA is inferior - $F_{max,epoxy} = 4.34$kN, $F_{max,PMMA} = 2.05$kN. The same is true for the absorbed energy – $E_{m,epoxy} = 2.23/11.52$J and $E_{m,PMMA} = 1.96/5.60$J for $< 45°$C/ $> 60°$C.
4) Twill glass fibre PMMA specimens perform nearly identically at room temperature while worse at temperatures $> 40°$C - $F_{max,epoxy} = 4.77/6.07$kN, $F_{max,PMMA} = 4.58/5.25$kN, $E_{m,epoxy} = 11.15/18.84$J and $E_{m,PMMA} = 8.19/11.47$J for </> $40°$C.
5) The experiment results align well with the analytic solution for the UD Carbon specimens. The enhancement of PMMA adhesion is clearly seen with the Force-Displacement curve being more straight in the elastic region and tracking the analytic solution line more precisely.
6) PMMA is thus from impact properties point of view a very suitable replacement for epoxy at temperatures $< 40°$C.

List of References

[1] Ming Yuan He; Anthony G. Evans; and John H. Hutchinson, **1994**, *Crack deflection at an interface between dissimilar elastic materials: role of residual stresses*, Int. J. Solids Structures Vol. 31, No. 24, pp. 3443·3455.

[2] McLaughlin, E. C.; Tait, R. A. *Fracture energy of plant fibres*, Journal of Materials Science, Volume 14, Issue 4, pp. 998-9, **1979**

[3] Lilholt, H. *Strengthening and its mechanisms*, Mechanical Properties of Metallic Composites — **1994**, pp. 389-471

[4] J. N. Kirk, M. Munrot, P.W.R. Beaumont *The fracture energy of hybrid carbon and glass fibre composites*, Journal of material science 13 **1978** 2197-2204

[5] J. O. Outwater and M. C. Murphy, *On the fracture energy of uni-directional laminates*, Spi Reinf Plast'compos Div, Proc 24th Annu Tech Conf — **1969**

[6] Konstantinos G. Dassios , *A review of the pull-out mechanism in the fracture of brittle matrix fibre-reinforced composites*, Advanced Composites Letters · January **2007**

[7] A. Kelly, N. H. Macmillan , *Strong solids*, Clarendon press, Oxford, **1986**

[8] A. Kelly, *Interface effects and the work of fracture of a fibrous composite*, Proc. Roy. Soc. Loud. A. 319, 95-116,**1970**

[9] H. L. Cox, *The elasticity and strength of paper and other fibrous materials*, British Journal of Applied Physics, Volume 3, Number 3, **1952**

[10] Aveston, J.; Kelly, A., *Theory of multiple fracture of fibrous composites*, Journal of Materials Science, vol. 8, issue 3, pp. 352-362, **1973**

[11] A.R. Bunsell, J. Renard, *Fundamentals of Fibre Reinforced Composite Materials*, Institute of Physics Publishing, Bristol, UK, **2005**

[12] X. Huang, *Fabrication and Properties of Carbon fibers*, Materials, **2009**

[13] D.J. Johnson, *Structure-property relationships in carbon fibres*, Appl. Phys. 20 286, **1987**

[14] *https://www.textiletoday.com.bd/an-overview-of-glass-fibers/*, visited on **2019/04/04**

[15] D. Hull, T. W. Clyne, *An introduction to composite materials*, Cambridge University Press, p. 150, **1996**

[16] *https://www.academia.edu/7463236/glass-fibres-manufacturing-properties-and-applications*, visited on **2019/04/05**

[17] *http://www.scielo.br/scielo.php?script=sci-arttext&pid=S0104-14282015000100002*, visited on **2019/04/05**

[18] H. Lilholt, B. Madsen *Properties of flax and hemp composites*, Flax and hemp fibres: a natural solution for the composites industry, JEC composites, Paris, France **2012**

[19] M. Kothe, C. Kothe, B. Weller *Epoxy resin adhesives for structural purposes – a new approach*, Conference: engineered transparencyAt: Düsseldorf, **2014**

[20] Van Rijswijk, K.; Bersee, H.E.N. *Reactive processing of textile fiber-reinforced thermoplastic composites—An overview*, A Appl. Sci. Manuf., 38, 666–681, **2007**

[21] Department of defence handbook *Composite materials handbook - Volume 3. Polymer matrix composites materials usage, design and analysis*, MIL-HDBK-17-3F Volume 3 of 5, **2012**

[22] A. Sindhuphak *Bioproducts of automotive accessories: Rethinking design materials through cornstarch, sugarcane and hemp*, **2007**

[23] S. Sakka *Effects of Reheating on Strength of Glass Fibers*, **1956**

[24] K. Yu, Q. Shi, M.L. Dunn, T. Wang *Carbon Fiber Reinforced Thermoset Composite with Near 100% Recyclability*, Adv. Funct.Mater. **2016**, 26, 6098–6106

[25] S. Timoshenko, S. Woinowsky-Krieger *Theory of plates and shells*, McGraw-Hill, **1959** - Science